university of groningen

The potential role of LPS dephosphorylation in preventing Necrotizing Enterocolitis

By

E.H.Buitenhuis

A Master's Thesis

Submitted to the Faculty of Science and Engineering

Biomedical sciences: Cancer and immune system

University of Groningen

June 2025

Supervised by Prof. Dr. K. Poelstra

SN: S3994538

Abstract

Necrotizing enterocolitis (NEC) is a severe intestinal disease primarily affecting preterm infants, characterized by intestinal inflammation, epithelial barrier disruption, and bacterial translocation. A key contributor of this pathology is lipopolysaccharide (LPS), a component of gram-negative bacteria that activates Toll-like receptor 4 (TLR4) on intestinal and immune cells. TLR4 proceeds through two distinct pathways: the MyD88-dependent and the TRIF-dependent pathway, generally being pro-inflammatory and anti-inflammatory respectively. Modulating this signaling balance may be critical for preventing or treating NEC.

In this study, we examined the effect of LPS, its lipid A component diphosphoryl lipid A (DPLA), and the dephosphorylated derivative monophosphoryl lipid A (MPLA) on epithelial barrier function and TLR4 signaling. Human colorectal adenocarcinoma cells (CaCo2) and rat intestinal epithelial cells (IEC6) were stimulated with LPS, DPLA, or MPLA and analyzed for changes in tight junction proteins via western blot and fluorescence microscopy. No significant disruption of tight junctions was observed, even at high LPS concentrations. To explore TLR4 signaling, mouse macrophage cells (RAW 264.7) were stimulated with LPS, DPLA, or MPLA, and cytokine expression was analyzed by qPCR. MPLA stimulation resulted in higher expression of TRIF-associated and lower expression of MyD88-associated cytokines compared to DPLA. These findings suggest that LPS dephosphorylation shifts TLR4 signaling toward a less inflammatory profile, which may reduce intestinal inflammation and epithelial damage, potentially contributing to the prevention or treatment of NEC.

Key words: Necrotizing enterocolitis, Lipopolysaccharide (LPS), Toll-like receptor 4 (TLR4), intestinal epithelium, MyD88/TRIF Signaling Pathways

Table of contents

1. Introduction

Necrotizing enterocolitis (NEC) is a severe gastrointestinal disease that primarily affects preterm infants. NEC has a total mortality rate of 23.5%, accounting for approximately 1 in 10 neonatal deaths (1). Even if the infants survive NEC, they still have a poor prognosis (2, 3). Among the many risk factors for NEC, the most prominent one is infant prematurity (4). This is thought to be due to the immature intestine and gastrointestinal immune system (5-8). In combination with a dysbiosis of the microbiome, this can lead to inflammation, necrosis, and perforation of the intestinal wall, eventually this may give rise to systemic inflammation (6-8).

One overlapping factor that plays a role in the pathophysiology of NEC is the Toll-like receptor 4 (TLR4). This receptor is capable of detecting lipopolysaccharide (LPS), which is a major component of the outer membrane of Gram-negative bacteria (9, 10). LPS consists of three main parts: lipid A, the core polysaccharide, and the O-antigen, which varies the most among bacterial species (11-13). The lipid A part is responsible for the endotoxicity, as this is the part that is recognized by the innate immune system (11). In the intestine, LPS binds to LPS binding protein (LBP), and is transferred to CD14, which in turn transfers LPS to the TLR4/MD2 complex on the surface of intestinal epithelial cells and immune cells (11, 14-16). This interaction activates two distinct intracellular pathways: the MyD88-dependent pathway and the TRIF-dependent pathway (17-19). The MyD88-dependent pathway promotes the production of pro-inflammatory cytokines such as TNF-α, IL-1β, and IL-6 (20,21), while the TRIF-dependent pathway produces anti-inflammatory cytokines like IFNβ and IL-10 (22-24). However, both pathways seem to converge on several key molecules, including NF-κB and MAPKs such as p38, thereby influencing a broad spectrum of immune and cell responses (24-26). This balance between the two pathways seems to be regulated by several molecules to induce appropriate responses to stimuli (27, 28). In the context of NEC, MyD88 signaling has been shown to drive inflammation and apoptosis, thereby contributing significantly to disease progression (29).

Beyond immune signaling, TLR4 activation has also been shown to negatively impact epithelial barrier function, primarily through the disruption of tight junctions (30-32). Tight junctions are protein complexes that maintain intestinal barrier integrity. These junctions consist of several proteins such as occludin, claudins, ZO-1, and cadherins (33). TLR4 signaling can alter both the expression and localization of these proteins, thereby disrupting tight junction integrity and increasing epithelial permeability (34-36). This disruption reduces the barrier function of the intestinal epithelium, allowing translocation of LPS and bacteria from the lumen into the bloodstream (37). This translocation can trigger systemic inflammation or sepsis, both key features in the pathophysiology of NEC(38, 39). Notably, TLR4 expression is upregulated in the intestinal epithelium of preterm infants compared to adults (40-42). Adding to this, preterm infants are more likely to develop a dysbiosis and are more susceptible to a dysbiosis of the microbiome, characterized by a decrease in beneficial bacteria and an increase in gram-negative

bacteria, leading to elevated luminal levels of LPS (35, 43-46). This combination of increased TLR4 expression and elevated luminal LPS levels may result in amplified TLR4 signaling. The interplay between these factors highlights the central role of TLR4 and LPS in the pathogenesis of NEC.

NEC treatment strategies have remained largely unchanged over the past decades due to all kinds of challenges, therefore mortality rates remain high (1, 47-49). Moreover, the global increase in the survival rates of preterm infants, as a result of improvements in neonatal care, may even be accompanied by a rise in the incidence of NEC (50, 51). Current therapeutic options are mostly supportive, including antibiotics, stopping enteral feeding, and simply monitoring. In more severe cases, surgery is needed (48, 49). Targeted modulation of the underlying pathophysiology remains a challenge. However, there is one consistent factor that seems to decrease NEC incidence. This is maternal breast milk (50-56). The exact reason why this happens is not quite known. It has been shown that human milk oligosaccharides and immunoglobulin A in breast milk protect against NEC (57, 58). However, this likely does not fully explain why maternal breast remains the most effective preventative measure for NEC.

One other important component of breast milk is alkaline phosphatase (59, 60). This enzyme can detoxify LPS by removing one of the two phosphate groups from the lipid A part of LPS, turning the lipid A into monophosphoryl lipid A (MPLA) (61). MPLA is known to be less toxic than LPS and can even be protective in some cases (61-65). To analyze the effects of lipid A dephosphorylation, MPLA can be compared to diphosphoryl lipid A (DPLA), which is the lipid A part of LPS retaining both phosphate groups (Fig. 1).

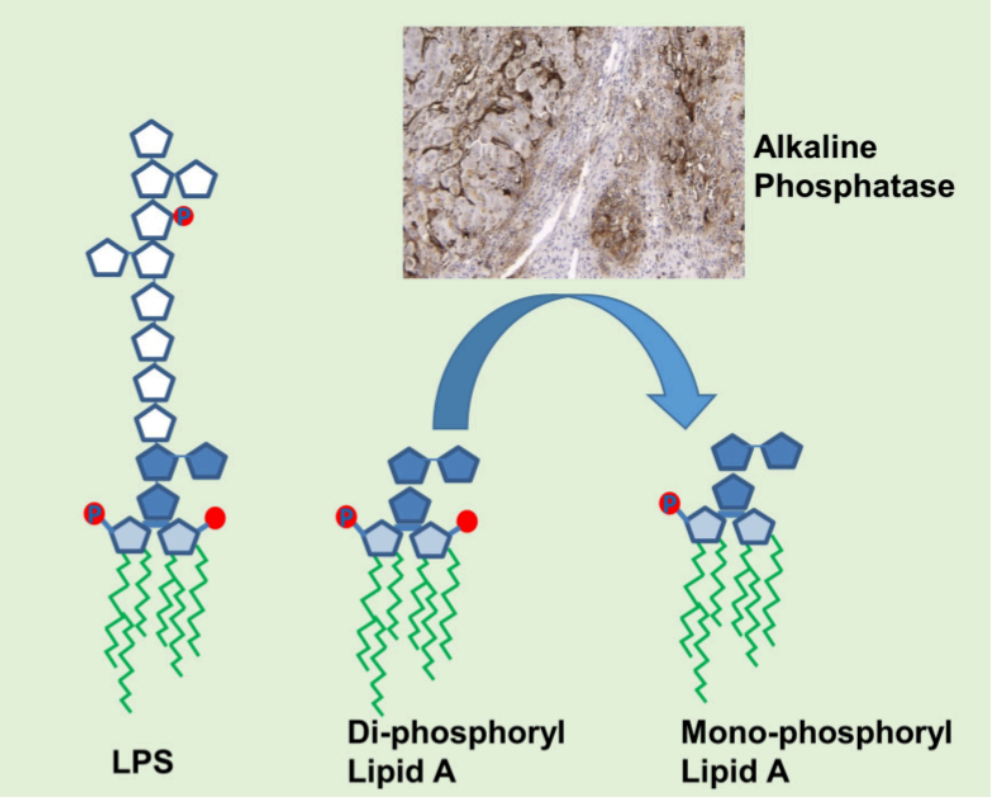

Fig 1. Graphical representation of LPS, DPLA and MPLA adapted and modified from Schippers et al. (2020) (66)

In this study, we hypothesized that MPLA has a reduced impact on tight junction disruption and promotes a more TRIF-dependent and less MyD88-dependent TLR4 signaling response compared to DPLA. This preservation of epithelial integrity, combined with a shift in TLR4 signaling, may contribute to the prevention of NEC by limiting translocation of LPS and bacteria from the lumen to the blood and reducing the pro-inflammatory MyD88-dependent response. To test this hypothesis, we investigated the effects of LPS on epithelial barrier function and TLR4 signaling, and whether these effects are altered when LPS is dephosphorylated.

To assess the effects of LPS and dephosphorylation of LPS on the intestinal barrier function, human colorectal adenocarcinoma cells (CaCo2) and rat intestinal epithelial cells (IEC6) were stimulated with LPS, DPLA, or MPLA to investigate changes in signaling pathways and epithelial integrity using western blot and fluorescence microscopy. To further explore specific TLR4 signaling pathways, mouse macrophage cells (RAW 264.7) were stimulated with LPS, DPLA, or MPLA, and cytokine profiles associated with the MyD88- and TRIF-dependent pathways were analyzed by qPCR.

2. Materials and Methods

2.1 Materials and chemicals

DMEM (32430-027 Gibco), FBS (S-FBS-SA-015, SERENA®), Pen/Strep (15140-122, Gibco), NEAA (11140-050, Gibco), Insulin (12585-014, Gibco), dPBS (14190-094, Gibco), TEP (15090-046, Gibco), Bürker counting chamber (Optik Labor), Gentamicin (15750-060, Gibco), Tetrazolium (M5655, Sigma), *Escherichia Coli* LPS O55:B5 (L2880, Sigma), *Klebsiella Pneumoniae* LPS (L4268, Sigma), *Salmonella Enterica* serotype typhimurium (L6511, Sigma), DPLA *Salmonella Enterica* serotype minnesota (L0774, Sigma), MPLA *Salmonella Enterica* serotype minnesota (401, List Labs), 1-Naphthyl)ethylenediamine dihydrochloride (222488, Sigma), Sulfanilamide (s9251, Sigma), EDTA (1.08418, MERCK), Lidocaine (L5647, Sigma), BSA (A9647, Sigma), Saponin (S7900, Sigma), formaldehyde (1.04003, Sigma), MaxWell simplyRNA kit (AS1280, Promega), RT buffer (M531A, Promega), Rev transcriptase (M170A, Promega), Rnasin® (N215B, Promega), dNTP (U151A, Promega), Random primers (C118A, Promega), GoTaq Master Mix® (A600A, Promega), Take 3 (TAKE3-SN, Agilent), Nuclease-Free water (P119E, Promega), Nitrocellulose membrane (1620115, Bio Rad), Molecular weight marker red (1610373, Bio Rad), Molecular weight marker all blue (1610374, Bio Rad), Powdered Milk (T145.2, ROTH), Alexa Fluor 488 (A-11008, Invitrogen), Alexa Fluor 647 (A32728, Invitrogen), Anti-Rabbit HRP (P0448, Agilent), Anti-Mouse HRP (P0260, Agilent), ZO-1 (61-7300, Invitrogen), Occludin (33-1500, Invitrogen), TLR4 (Western blot, ab22048, Abcam), TLR4 (flow cytometry, ab13556, Abcam), TLR4 (Confocal microscopy, MA5-16216, Invitrogen), β-actin (4970, Cell Signaling), p38 (9212, Cell signaling), P-p38 (4631, Cell Signaling), P-NF-kB (3033, Cell Signaling).

2.2 Cell cultures

All cells were cultured in 25 or 75 cm² flasks at 37℃ under humidified atmospheric conditions containing 5% CO_2. Cells were counted using a Bürker counting chamber.

The CaCo2 cells (passage 27) were cultured in a DMEM medium containing 10% FBS, 1% NEAA, and 1% Pen/Strep. Culture medium was changed every 2-3 days. Cells were passaged when confluency reached 80%. For passaging, cells were washed twice with dPBS and trypsinized with TEP. After trypsinization, cells were centrifuged at 300g for 5 minutes to remove all TEP left in the culture medium.
CaCo2 cells can be further differentiated for approximately 21 days, during which they develop more epithelial-like characteristics. To create 21 days differentiated CaCo2 cells, Caco2 cells were kept confluent for 21 days, and the medium was replaced every 2-3 days.

The IEC6 cells (passage 12) were cultured in a DMEM medium containing 10% FBS, 1% Pen/Strep, and 0.37% insulin. Culture medium was changed every 3-4 days. Cells were passaged before reaching confluency. For passaging, cells were washed twice with dPBS and trypsinized with TEP. After trypsinization, cells were centrifuged at 300g for 5 minutes to remove all TEP left in the culture medium.

The RAW 264.7 cells (passage 8) were cultured in a DMEM medium containing 10% FBS and 0.024% Gentamicin. Culture medium was changed every 2-3 days. Cells were passaged before reaching 90% confluency. For passaging, cells were collected using a cell scraper and centrifuged at 300g for 5 minutes to remove debris and dead cells.

2.3 Treatments

The main treatments used in this study included various concentrations of LPS, DPLA, and MPLA. Concentration ranges were selected based on previous work by colleagues as well as published literature. Where possible, clinically relevant concentrations (1-10ng/ml) were used (35). However, higher concentrations were applied in most experiments to induce a cellular response. For RAW 264.7 cells, treatment concentrations were 100ng/ml. For CaCo2 and IEC6 cells, treatment concentrations ranged from 1-10 µg/ml, based on multiple publications that use these concentrations (67-69). Unless otherwise stated, all LPS used were derived from *Escherichia coli*.

2.4 MTT assay

To assess cytotoxicity and evaluate cell viability in CaCo2 cells following LPS treatment, an MTT assay was performed. This assay measures the conversion of the MTT dye by mitochondrial enzymes, making it an indicator of metabolic activity and thus cell viability. CaCo2 cells were seeded onto 96-well plates at a density of 2×10^5 cells/cm^2. After 24 hours, incubation medium was replaced with treatment containing medium consisting of: 1µg/ml LPS,

50ng/ml IFNγ, 1µg/ml LPS + 50ng/ml IFNγ, 10% DMSO, or 50% MDSO. Each treatment had 3 replicates. After 24 hours incubation, 100µl of medium was taken for NO assay. The rest of the medium was removed and cells were washed with PBS. After washing, cells were incubated with 200µl 0.5mg/ml Tetrazolium in medium for an hour, then replaced with 100µl DMSO and put on a shaker until all crystals were dissolved. The absorbance was measured at 550nm wavelength using the Synergy H1 microplate reader**.**

2.5 Nitric Oxide (NO) assay

Nitric oxide (NO) production is one of the many cellular responses to inflammation and TLR4 activation. It is easily quantifiable and measurable via nitrite accumulation in the medium. It is used to measure CaCo2 cell response to LPS, and to measure RAW 264.7 cell response to LPS, DPLA, and MPLA.

For CaCo2, the medium used for NO measurement was collected as described in the MTT assay section.

RAW 264.7 cells were seeded onto 96-well plates at a density of 2.5×10^5 cells/cm^2. After 24 hours incubation, the medium was replaced with treatment containing medium consisting of 100ng/ml LPS, DPLA, or MPLA and incubated for 18 hours. Each treatment was performed in 2 or 3 replicates. To determine the level of nitrite in the culture medium, 100µl of Griess reagent (sulfanilamide, phosphoric acid, N-(1-Naphthyl)ethylenediamine dihydrochloride in milli-Q water) was added to 100µl medium of the sample. Absorbance was measured at 550nm using the Synergy H1 microplate reader.

2.6 Protein extraction and western blot

Western blotting is a widely used technique to detect specific protein expression and phosphorylation of proteins. It allows for qualitative and semi quantitative assessment of protein levels in response to treatments. It is used to measure tight junction protein levels in CaCo2 and IEC6 cells.

Proteins were extracted using a RIPA lysis buffer (containing RIPA buffer, protease inhibitor cocktail, Sodium orthovanadate, NaF, Phosphostop). Genomic DNA was sheared using an insulin needle. Equal volumes of protein lysates were loaded onto SDS-PAGE gel alongside a molecular weight marker. After electrophoresis, proteins were transferred onto a nitrocellulose membrane. Membranes were blocked with 5% skimmed milk and incubated overnight with primary antibodies: β-actin (1:5000), Occludin (1:1250), ZO-1 (1:2500), TLR4 (1:1000), p38 (1:2500), P-p38 (1:2500), P-NF-kB (1:2500) and IL-1β (1:1250). Species matched HRP-conjugated secondary antibodies were used (1:2500) for detection. Then Amersham™ ECL prime western blotting detection reagent was added on the membrane and the bands were detected by the Uvitec Alliance Q9. Bands were quantified using the Ninealliance software. All data were normalized by β-actin.

2.7 Confocal microscopy

Confocal microscopy is a powerful imaging technique that can be used to visualize fluorescently labeled cellular structures with high resolution. It enabled the visualization of tight junction protein in CaCo2 and IEC6 cells in response to LPS.

CaCo2 and IEC6 cells were seeded onto 96-well plates at a density of 1.5×10^5 and 2×10^4 cells/cm^2 respectively, and grown over the weekend to allow the cells to reach confluence and establish tight junctions. After 72 hours, cells were stimulated for 48 hours with treatments. Treatments consisted of different concentrations of LPS (10ng/ml - 10µg/ml), and different LPS species *(*derived from *Escherichia coli, Klebsiella Pneumoniae*, and *Salmonella enterica*). After 48 hours, cells were washed twice with PBS, fixed with 4% formaldehyde, permeabilized with 1mg/ml saponin, and blocked with 3% BSA. Cells were then incubated with primary antibodies Occludin (1:120), ZO-1 (1:120), or TLR4 (1:60). Subsequently, they were incubated with secondary antibodies Alexa Fluor 647 (1:60) and Alexa Fluor 488 (1:60). Nuclei were stained with 10µg/ml Hoechst 33342. Fluorescent signals were visualized using the Zeiss CD7 confocal microscope.

2.8 Flow cytometry

Flow cytometry is a method used to measure proteins on the surface of cells using fluorescent labels. It was used to measure TLR4 expression on RAW 264.7 cells.

RAW 264.7 cells were seeded onto 12-well plates at a density of 4×10^4 cells/cm^2 and incubated for 48 hours before being harvested with an EDTA/lidocaine solution (EDTA, lidocaine, and FBS in PBS). Cells were counted and reseeded onto a 96-well plate at a density of 5×10^4 cells/well. Cells were stained with primary antibody TLR4 (1:100), followed by the secondary antibody Alexa Fluor 488 (1:250). Between each step, cells were washed with a staining buffer (EDTA and FBS in PBS) and centrifuged at 300g for 5 minutes. Finally, cells were transferred to flow cytometry tubes and analyzed using the CytoFLEX S. Data were analyzed by FlowJo v10.

2.9 RNA extraction and qPCR

Quantitative PCR (qPCR) was used to assess changes in cytokine mRNA expression related to MyD88- and TRIF-dependent signaling following treatment with LPS, DPLA, or MPLA.

RAW cells were seeded onto 12-well plates at a density of 4×10^4 cells/cm^2. After 24 hours, cells were treated with 100ng/ml LPS, DPLA, or MPLA for different times (1-24 hours). RNA was isolated using the Maxwell® RSC simplyRNA cells kit according to the manufacturer's instructions. RNA concentration was measured with the Take3 device and converted into cDNA using an in-house prepared RT mix (RT buffer, dNTP mix, Rnasin®, Rev transcriptase, Random hexamers, nuclease-free water). qPCR was performed with GoTaq® Master Mix and custom primers (listed in Table 1) on a Quantstudio 7 Flex System. Gene expression was quantified absolutely using standard curves and normalized to β-actin in QuantStudio v1.7.2.

Gene	Forward (5′-3 ′)	Reverse (5′-3′)
β-actin	ATCGTGCGTGACATCAAGA	ATGCCACAGGATTCCATACC
TNF-α	CATCTTCTCAAAATTCGAGTGACAA	GAGTAGACAAGGTACAACCC
IL-1β	GCCAAGACAGGTCGCTCAGGG	CCCCCACACGTTGACAGCTAGG
IL-10	ATAACTGCACCCACTTCCCAGTC	CCCAAGTAACCCTTAAAGTCCTGC
IFNβ	CGTGGGAGATGTCCTCAACT	CCTGAAGATCTCTGCTCGGAC

Table 1. Primers used for qPCR in this study.

2.10 Statistical analysis

Most experimental data were analyzed using Excel. For qPCR data, an additional analysis was performed using R Studio. Data are presented as mean ± standard deviation (SD) where possible. Differences between groups were assessed using an unpaired two-sample t-test assuming unequal variances. P values < 0.05 are considered statistically significant.

3. Results

3.1 Verification of TLR4 expression in CaCo2, IEC6 and RAW264.7 cells

To establish the relevance of the selected cell lines for studying the impact of LPS on tight junctions and TLR4-mediated signaling, TLR4 expression was verified, as TLR4 is the primary receptor responsible for recognizing LPS. Without TLR4 expression, cells cannot mount a response to LPS.

TLR4 protein expression was confirmed for both undifferentiated and differentiated CaCo2 via western blotting (Fig. 2A). Note that the difference in band intensity between these conditions does not reflect biological differences, as unequal protein amounts were loaded. Additionally, TLR4 expression was visualized in IEC6 cells and CaCo2 cells using confocal microscopy (Fig. 2B). For RAW264.7 cells, TLR4 protein could not be detected by western blot, but flow cytometry confirmed TLR4 surface expression (Fig. 2D).

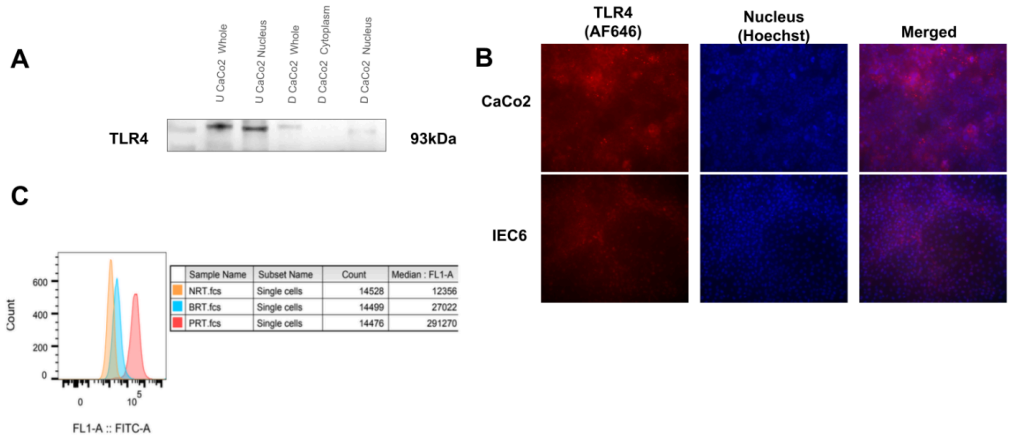

Fig 2. TLR4 expression in RAW, CaCo2 and IEC6 cells.
(A) TLR4 expression on CaCo2 cells measured by western blot (U= undifferentiated, D = differentiated). **(B)** TLR4 expression on CaCo2 and IEC6 cells measured by confocal microscopy. **(C)** Histogram showing TLR4 expression on RAW cells measured by flow cytometry

3.2 Impact of LPS on nitric oxide production and cell viability in CaCo2 cells

To evaluate whether intestinal epithelial cells respond to LPS, a nitric oxide (NO) assay was performed following 24-hour stimulation of confluent CaCo2 cells with LPS (1µg/ml) and or IFNγ (50ng/ml). IFNγ was included to determine whether co-stimulation is required to induce a cellular response to LPS. NO production was not detected in any treatment group, indicating that CaCo2 cells do not produce NO under these conditions (Fig. 3A). To assess the impact of LPS on cell viability in intestinal epithelial cells, an MTT assay was performed using the same treatment groups in CaCo2 cells. LPS alone had a slight effect on cell viability, while co-treatment with IFNγ appeared to further reduce cell viability slightly. However, these changes were marginal. Interestingly, treatment with 10% DMSO, intended as a negative control, resulted in an unexpected increase in cell viability compared to untreated controls. Therefore, 50% DMSO was included as an additional condition, which effectively killed all cells and thus served as a more appropriate negative control (Fig. 3B). Microscopic imaging supported these findings. No clear difference in MTT staining or cell morphology was observed between control and LPS-treated cells. The increase of MTT staining for 10% DMSO was clearly visible. Interestingly, there appeared to be more gaps between the cells in 10% DMSO compared to 50% DMSO (Fig. 3C).

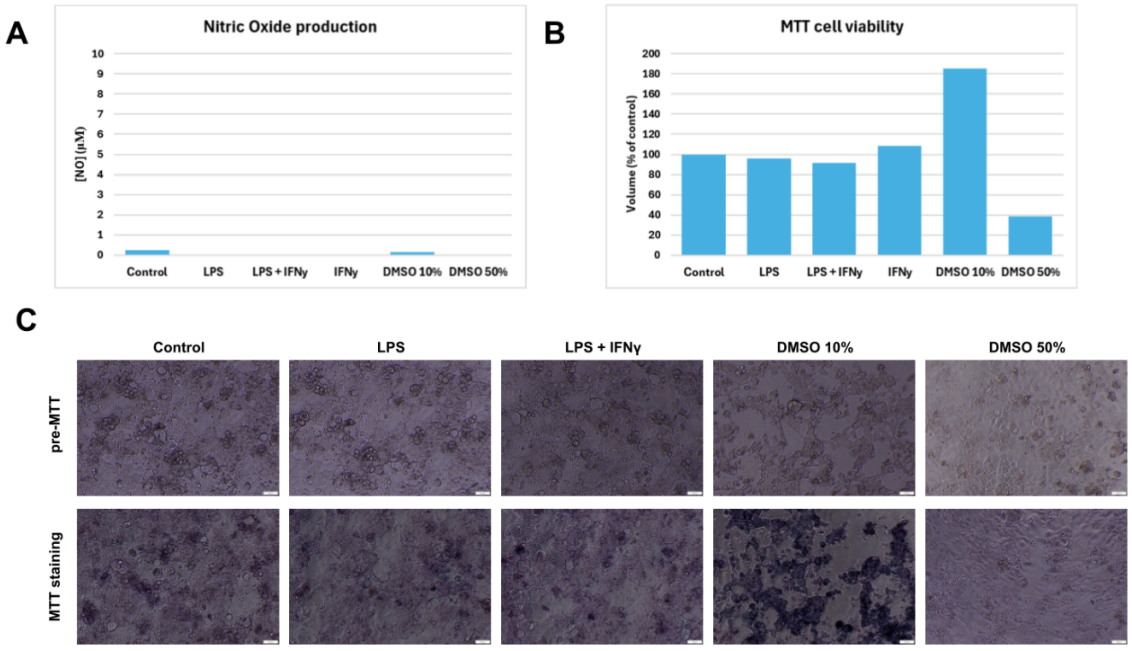

Fig 3. Effect of LPS on NO production and MTT cell viability
(A) Nitric Oxide production of CaCo2 cells as measured by Nitric Oxide assay. (LPS = 1µg/ml, IFNγ = 50ng/ml) **(B)** Cell viability of CaCo2 cells measured by MTT assay. **(C)** Pictures of cells before and after MTT assay.

3.3 Which signaling cascades are activated by LPS in CaCo2 cells?

To explore which signaling pathways are activated by LPS in CaCo2 cells, phosphorylation targets of key TLR4 downstream targets were investigated. In specific, NF-κB and MAPK p38 phosphorylation are promising targets according to literature (24-26, 67). CaCo2 cells were stimulated with 1µg/ml LPS for 10, 20, and 60 minutes, and phosphorylated protein levels were analyzed by western blot. LPS treatment did not increase NF-κB phosphorylation at any time point compared to control (Fig. 4A). In contrast, p38 phosphorylation showed a time-dependent increase following LPS stimulation, while total p38 levels remained unchanged (Fig. 4B), suggesting p38 activation. Based on these results, subsequent experiments focused on p38 phosphorylation. To determine an appropriate LPS concentration, cells were treated with 10 ng/ml or 1 µg/ml LPS. Both concentrations induced similar levels of p38 phosphorylation (Fig. 4C,D), so 10 ng/ml was selected for further experiments as it is more physiologically relevant. To investigate whether p38 phosphorylation is altered by LPS dephosphorylation, p38 phosphorylation was compared after treatment with LPS, DPLA, or MPLA. After 20 minutes 10 ng/ml stimulation, MPLA induced slightly less p38 phosphorylation compared to LPS and DPLA (Fig. 4E,F). To ensure that observed effects were not caused by cellular stress from medium replacement, treatments were also added directly to existing medium, and time-matched controls were included for each time point. At 10 ng/ml, LPS, DPLA, and MPLA did not change p38 phosphorylation compared to control. Increasing the dose to 1 µg/ml still did not affect p38 phosphorylation at 10 and 20 minutes. However, after 60 minutes, all treatments appeared to increase p38 phosphorylation (Fig. 4G,H), suggesting delayed phosphorylation of p38.

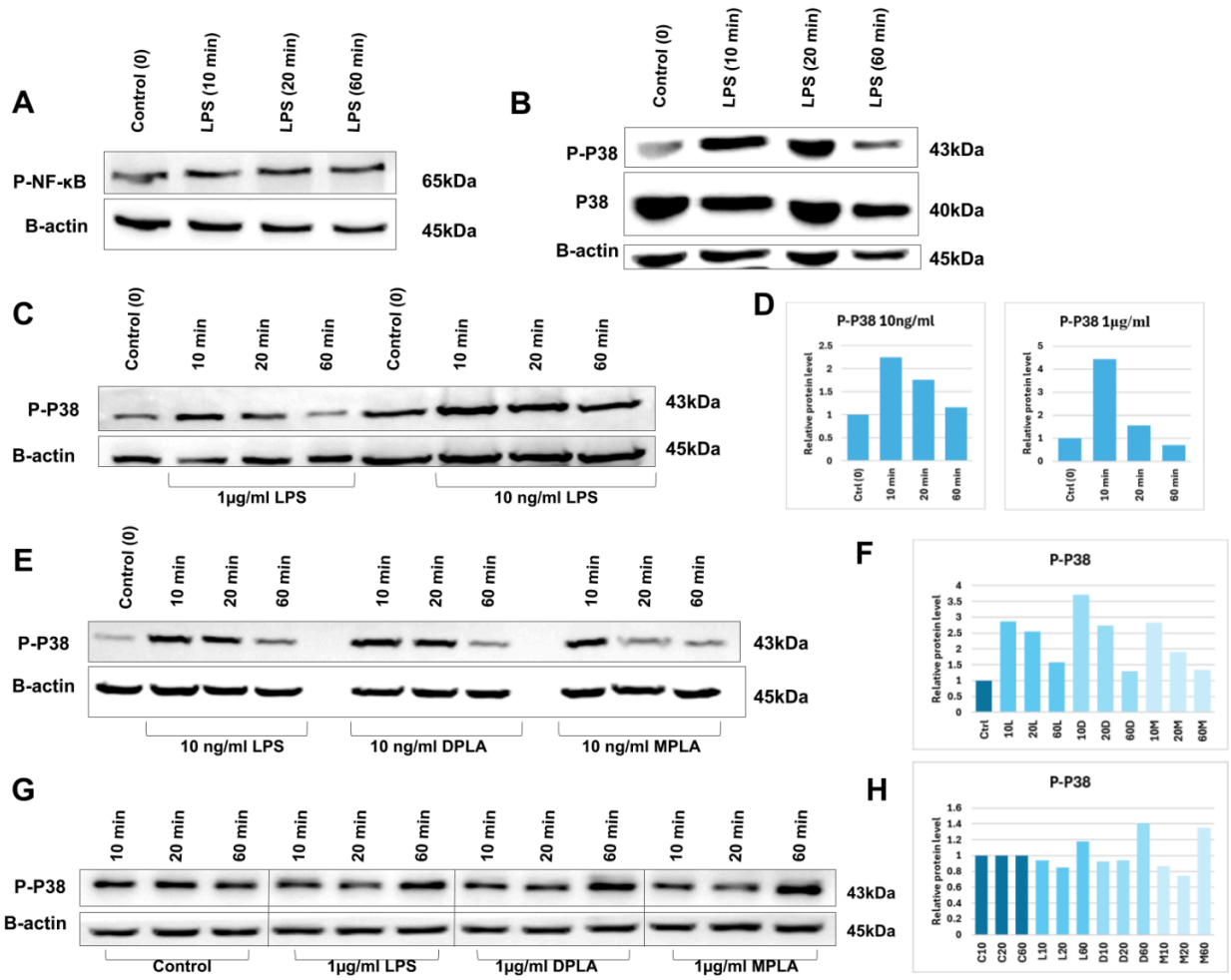

Fig 4. P38 phosphorylation after LPS, DPLA, or MPLA stimulation in CaCo2 cells
Phosphorylation was all measured by western blot in CaCo2 cells. For A-F cells were treated by replacing medium with treatment. For G treatment was directly added to existing medium.
(A) Effect of a time dependent LPS stimulation on NF-κB phosphorylation (LPS = 1µg/ml) **(B)** Effect of a time dependent LPS stimulation on P38 and P38 phosphorylation (LPS = 1µg/ml) **(C)** Comparison of time dependent LPS concentration impact on P38 phosphorylation. **(D)** Quantification of western blot (C). **(E)** Comparison of LPS, DPLA and MPLA and the time dependent effect on P38 phosphorylation. **(F)** Quantification of western blot (E), normalized by B-actin. **(G)** Comparison of control, LPS, DPLA and MPLA and the time dependent effect on P38 phosphorylation. **(H)** Quantification of western blot (H). Data is normalized by B-actin.

3.4 Impact of LPS on tight junction proteins in CaCo2 cells

To investigate whether LPS affects tight junction integrity in epithelial intestinal cells, CaCo2 cells were treated with 10ng/ml or 1µg/ml LPS for 24 hours. Western blot analysis showed no change in ZO-1, E-cadherin, or Occludin protein levels compared to untreated controls (Fig. 5A,B). Extending the incubation to 48 hours with 1 µg/ml LPS also did not reveal any time-dependent effect (Fig. 5C,D). Additionally, IL-1β levels were assessed to evaluate cytokine production, but no significant induction was observed. To validate these findings, CaCo2 cells were treated with 10 ng/ml, 1 µg/ml, or 10 µg/ml LPS for 48 hours, and confocal microscopy was used to assess fluorescence intensity and localization of ZO-1 and Occludin (Fig. 5E). No noticeable differences in fluorescence intensity or localization were observed between treated and untreated cells.

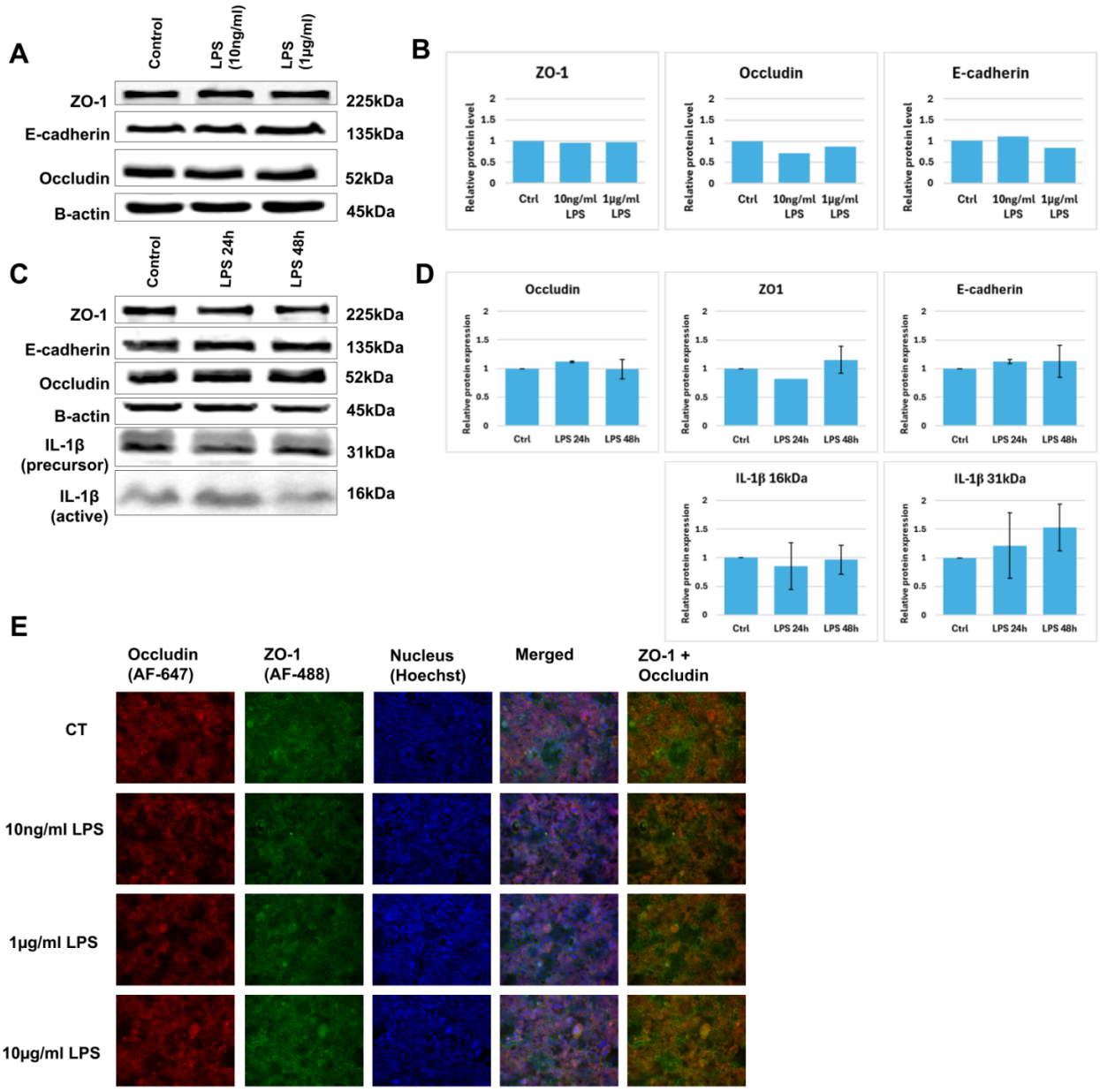

Fig 5. Impact of LPS on tight junctions in CaCo2 cells
(A) Western blot showing dose dependent effects of LPS treatment for 24 hours on tight junction proteins. **(B)** Quantification of western blot (A) (n=1). **(C)** Western blot showing the time dependent effect of LPS treatment on tight junction proteins and pro-inflammatory cytokine IL-1β (LPS = 1µg/ml) **(D)** Quantification of western blot (C), LPS 24 h: n=2 (ZO-1: n=1), LPS 48 h: n=5. **(E)** Confocal microscopy showing dose dependent effects of LPS treatment for 48 hours on tight junction proteins. Data is normalized by B-actin. No significant differences were observed, as determined by unpaired two-sample t-test.

3.5 Impact of LPS, DPLA, and MPLA on tight junction proteins in differentiated CaCo2 cells

CaCo2 cells can be differentiated to attain a more intestinal epithelial-like phenotype. Since both undifferentiated and differentiated CaCo2 cells are used in literature, we investigated whether differentiation affects treatment outcomes. CaCo2 cells were cultured for 21 days in 12-well plates and subsequently treated with 1 µg/ml LPS, DPLA, or MPLA for 48 or 72 hours. Tight

junction proteins ZO-1 and Occludin were analyzed via western blot and quantified (Fig. 6A,B). Results varied across experiments. In most cases, LPS reduced the expression of ZO-1 and Occludin compared to control. However, the effects of DPLA and MPLA were inconsistent; in some blots, expression levels were lower than control, while in others, they were elevated. On average, DPLA and MPLA did not show a clear or consistent impact on tight junction protein levels (Fig. 6B).

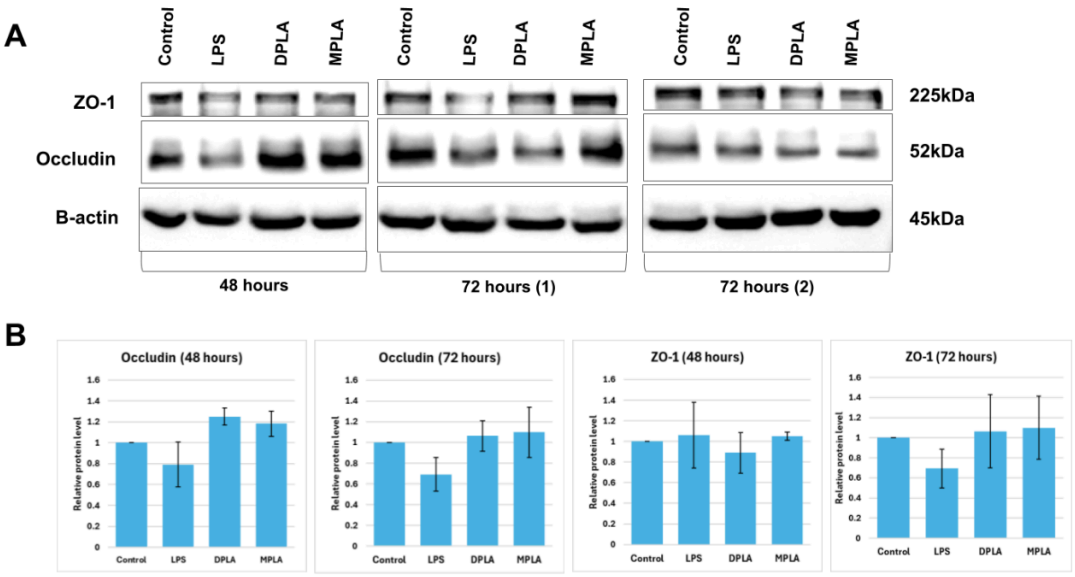

Fig 6. Impact of either LPS, DPLA, or MPLA on tight junctions in 21 days differentiated CaCo2 cells. **(A)** 21 days differentiated CaCo2 cells treated for 48 or 72 hours with either LPS, DPLA or MPLA. Protein level of ZO-1 and Occludin was measured by western blot. (1) = cells were treated by adding treatment directly to medium. (2) = cells were treated by replacing medium with medium containing treatment (Treatment concentration 1µg/ml).**(B)** Quantification of western blots (A). Data are shown for 48h (n=2) and 72h (n=3). Data is normalized by B-actin. No significant differences were observed, as determined by unpaired two-sample t-test.

3.6 Effects of different LPS species on tight junctions in IEC6 cells

Since LPS treatment did not affect tight junction proteins in CaCo2 cells as expected, we investigated whether a similar pattern occurs in IEC6 cells. Confocal microscopy was used to assess ZO-1 and Occludin fluorescence intensity as indicators of tight junction integrity. No clear effect was observed on ZO-1 fluorescence. Interestingly, Occludin fluorescence appeared to increase after LPS treatment compared to untreated controls, which showed relatively low baseline intensity (Fig. 7C). To determine whether this effect is specific to a particular LPS species, IEC6 cells were treated with LPS derived from *Escherichia coli*, *Klebsiella pneumoniae*, and *Salmonella enterica*. Western blot and confocal microscopy showed no consistent change in ZO-1 levels across LPS species (Fig. 7A,D). However, an increase in Occludin was again observed upon LPS treatment (Fig. 7A,D). Notably, the western blot signal appeared at ~30 kDa rather than the expected 52 kDa for Occludin. This lower band was inconsistent across

experiments, sometimes increased, sometimes unchanged, and other times differing between LPS species. A data based average showed an increase in Occludin for *E.coli, Klebsiella,* and DPLA, the ZO-1 level seems to vary around the control level, with no clear differences (Fig. 7B).

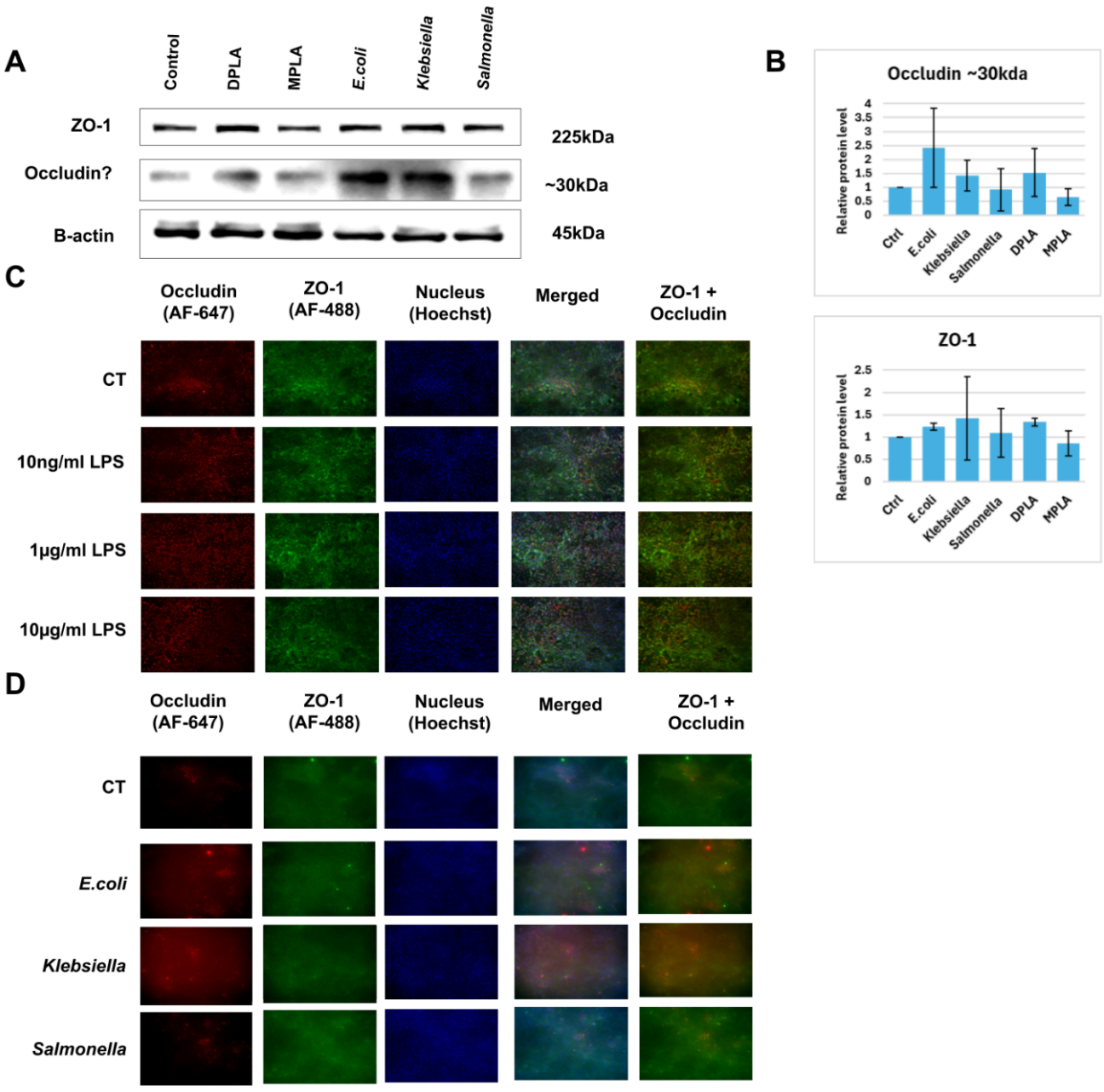

Fig 7. Impact of different LPS species on tight junctions in IEC6 cells
(A) IEC6 cells treated with DPLA, MPLA or different LPS species and the effect on ZO-1 and Occludin (Treatment concentration = 1µg/ml). **(B)** Quantification of western blot, data normalized by B-actin (n=3). **(C)** Confocal microscopy showing dose dependent effect of LPS on Occludin and ZO-1. **(D)** Confocal microscopy showing the effect of different LPS species on ZO-1 and Occludin in IEC6 cells (LPS = 10µg/ml)

3.7 Specific MyD88- and TRIF-Dependent pathway activation after LPS, DPLA, or MPLA treatment in RAW 264.7 Cells

To determine whether dephosphorylation of LPS alters TLR4 signaling, the expression of cytokines linked to the MyD88 and TRIF pathways was measured by qPCR after treatment with LPS, DPLA, or MPLA in RAW 264.7 mouse macrophage cells. TNFα and IL-1β represent pro-inflammatory MyD88-dependent cytokines, while IL-10 and IFNβ correspond to anti-inflammatory TRIF-dependent cytokines. A nitric oxide (NO) assay was first conducted to verify RAW 264.7 cell responsiveness to 100 ng/ml LPS, DPLA, and MPLA after 18 hours. LPS strongly induced NO production, followed by a moderate response to DPLA and a weaker response to MPLA (Fig. 8A). To identify optimal time points for cytokine mRNA measurement, cells were incubated with 100 ng/ml LPS for 1, 2, 18, or 24 hours. TNFα, IL-10, and IFNβ peaked early at 1 or 2 hours, while IL-1β peaked later at 18 hours (Fig. 8B). Based on these results, subsequent experiments used 1 and 18 hour time points for treatments with LPS, DPLA, or MPLA. Compared to untreated controls, all cytokines showed induction except IL-10, which remained largely unchanged (Fig. 8C). After 1 hour, MPLA treatment resulted in decreased TNFα and increased IL-1β and IFNβ compared to DPLA. After 18 hours, IL-1β expression in MPLA-treated cells returned nearly to baseline, contrasting with high IL-1β levels in DPLA-treated cells. TNFα remained lower in MPLA-treated cells, and IFNβ levels also returned to control levels (Fig. 8C). Overall MPLA-treated RAW 264.7 cells expressed less MyD88-dependent cytokines and a relative increase in TRIF-dependent cytokines compared to DPLA treatment.

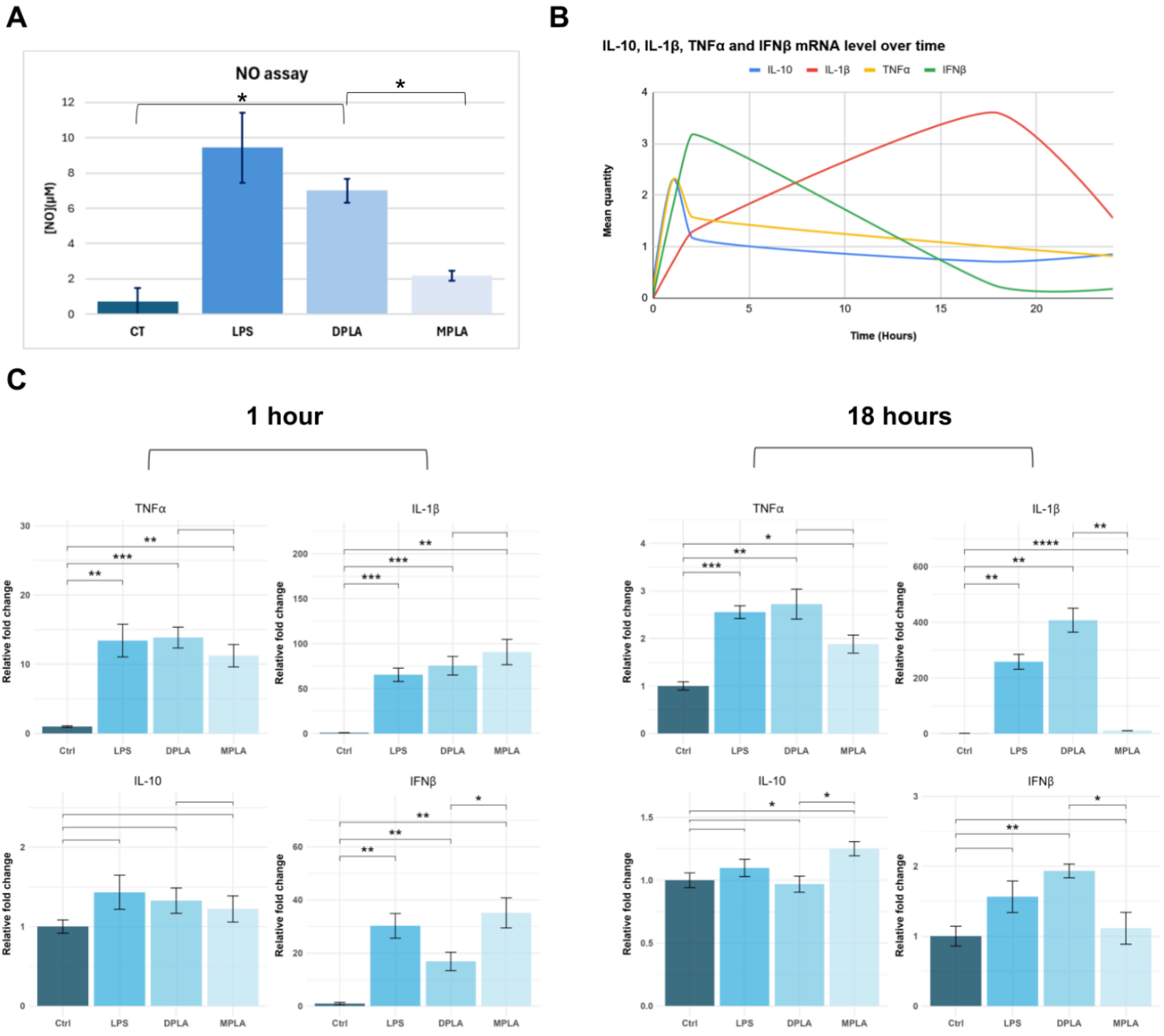

Fig 8. LPS, DPLA or MPLA treatment and its impact on mRNA expression of TRIF vs MyD88 related cytokines in RAW 264.7 cells

(A) NO assay showing the effect of 18 hour LPS, DPLA or MPLA treatment on NO production in RAW cells (n=2). **(B)** Timeline of qPCR results showing the effect of LPS on time specific mRNA expression of TNFα, IL-1β, IL-10 and IFNβ in RAW cells (n=1). Timepoints are 1, 2, 18 and 24 hours. Data is normalized by B-actin. **(C)** qPCR results showing the effect of LPS, DPLA or MPLA treatment on TNFα, IL-1β, IL-10 and IFNβ in RAW cells. Two timepoints taken, 1 hours (n=3) and 18 hours (n=2). Data is normalized by B-actin. All treatment concentrations are 100ng/ml. Statistical significance: * $p < 0.05$, ** $p < 0.01$, *** $p < 0.001$.

4. Discussion

4.1 Summary of results

This study aimed to determine whether MPLA has a reduced impact on tight junction disruption and induces a more TRIF-dependent and less MyD88-dependent TLR4 signaling compared to LPS, to explore the potential role of LPS dephosphorylation in preventing NEC. To assess the effect on tight junctions, two intestinal epithelial cell models were used: CaCo2 and IEC6 cells. Although CaCo2 cells express TLR4, they did not exhibit clear activation upon LPS stimulation. LPS was used to attempt disruption of the tight junctions, which was assessed by measuring ZO-1 and Occludin protein levels through western blot and confocal microscopy. However, we were unable to induce clear tight junction disruption in either cell model. Interestingly, in IEC6 cells, the typical 65kDa occludin band was not observed, instead, a lower molecular weight band at approximately 30kDa was detected, which increased in intensity following stimulation with *E.coli* or *Klebsiella*-derived LPS. The literature shows variability in the use of differentiated versus undifferentiated CaCo2 cells as a model. In our hands these differentiated cells also produced inconsistent results. In some cases we observed a reduction in ZO-1 and Occludin expression, but overall these differences were not statistically significant.

To assess the impact on TLR4 signaling, RAW 264.7 cells were used as a model for immune cell responses. These cells were activated by LPS, DPLA, and MPLA, as shown by NO production, which followed a decreasing trend from LPS to DPLA to MPLA. To determine which specific intracellular TLR4 pathway was activated, cytokines associated with MyD88 (TNFα, IL-1β) and TRIF (IL-10, IFNβ) signaling were measured using qPCR. TNFα, IL-10, and IFNβ are early responders, peaking at 1-2 hours, while IL-1β is a late responder, peaking at 18 hours. MPLA stimulation appeared to favor a more TRIF-dependent and less MyD88-dependent signaling profile. IL-1β expression was nearly absent at 18 hours following MPLA treatment, while it remained elevated in response to DPLA. MPLA also induces slightly lower TNFα expression at both 1 and 18 hours compared to DPLA. Lastly, IFNβ expression was higher at 1 hour in MPLA-treated cells compared to DPLA-treated cells. These findings suggest that dephosphorylation of LPS, resulting in MPLA, leads to a more anti-inflammatory signaling profile compared to DPLA.

4.2 Lack of CaCo2 cell activation

Despite the presence of TLR4 expression, CaCo2 cells did not show clear activation in response to LPS in our NO and MTT assays. This is partially consistent with the literature, while our MTT assay aligns with previous findings showing limited decreased cell viability in CaCo2 cells responding to LPS, the lack of NO production contrasts with some reports that do show NO production in CaCo2 cells (70, 71). Other studies have also reported LPS-induced phosphorylation of p38 in CaCo2 cells (67). Initially, we believed we had confirmed this p38 phosphorylation, but further experiments revealed that medium replacement alone was sufficient

to trigger this phosphorylation. This suggests that the effect was due to cellular stress rather than treatment (72). In follow-up experiments, where treatment compounds were added directly to the existing medium and timepoint-specific controls were included, we observed a potential increase in p38 phosphorylation after 60 minutes of incubation with LPS, DPLA, and MPLA. Suggesting a later phosphorylation than we initially expected. However, no significant differences were detected between the three treatments. It is possible that peak phosphorylation occurs after 60 minutes, as another study observed p38 phosphorylation following 4 hours incubation with LPS (83). Therefore, future experiments should include extended treatment durations to capture potential differences between treatments.

4.3 Tight junctions in CaCo2 cells

We were unable to consistently detect disruption of tight junction proteins ZO-1 and Occludin in CaCo2 cells, despite testing multiple timepoints (24, 48, and 72 hours) and a range of LPS concentrations (10ng/mL, 1 μg/mL, 10 μg/mL). Although occasional changes were observed, these differences were not statistically significant. Similar results were obtained in 21 days differentiated CaCo2 cells, where some experiments showed slightly more indication of tight junction disruption, yet overall results remained inconsistent and non-significant. This is in contrast to several published studies showing LPS-induced disruption of tight junctions. Important to note is that the severity of this disruption changes between these studies as well (64, 67, 73). These discrepancies may be attributed to several factors: The known variability in CaCo2 cell behavior between laboratories (74), differences in LPS source, serotype, concentration, and exposure time, as well as variations in seeding densities and culture conditions. Another possible explanation is that our CaCo2 cells express low levels of TLR4 or its co-receptors (such as MD-2 and CD14), which are essential for robust LPS recognition and downstream signaling. We did not check if the co-receptors are on the cells. Additionally, we did not assess the differentiation status of our differentiated CaCo2 cells. It is worth noting that the most effective method for achieving proper CaCo2 differentiation is culturing them on filter inserts, which more accurately mimic the polarized intestinal epithelium (75). Since our differentiated CaCo2 cells were not cultured under these conditions, their differentiation may have been incomplete, potentially contributing to the limited response to LPS observed in our experiments.

4.4 Tight junctions in IEC6 cells

To address the variability observed in CaCo2 cell responses and examine whether different LPS species have distinct effects, we evaluated tight junction integrity in IEC6 cells treated with LPS derived from *E.coli, Klebsiella,* and *Salmonella.* ZO-1 levels showed no consistent or significant changes compared to controls. Interestingly, the expected full-length Occludin band at 65kDa was mostly absent, instead, we observed a more distinct band at approximately 30kDa. This band increased in intensity after DPLA and LPS derived from *E.Coli* or *Klebsiella* treatment. This suggests possible Occludin degradation or the expression of an alternative isoform. Occludin is

known to have multiple isoforms resulting from (hyper)phosphorylation or alternative splicing (76). Notably, a type III splice variant of Occludin has been described with a molecular weight of 32.2 kDa. This variant lacks the fourth transmembrane domain, which prevents its co-localization with ZO-1 (77). As occludin and ZO-1 normally interact for proper tight junction function, this disruption could negatively impact tight junction integrity. Notably, the intensity of the band remained similar to control levels following MPLA treatment. If this lower occluding band indeed corresponds to the type III splice variant, it may suggest that LPS dephosphorylation can prevent Occludin disruption and potentially preserve barrier function.

4.5 TLR4 signaling in RAW 264.7 cells

Our findings in RAW 264.7 cells offer insights into the balance between the MyD88- and TRIF-dependent TLR4 signaling pathways. LPS, DPLA, and MPLA all activated TLR4, as shown by NO production, with decreasing potency from LPS to DPLA to MPLA. Gene expression analysis by qPCR revealed that MPLA induced lower levels of MyD88-associated cytokines (TNF-α and IL-1β), while enhancing TRIF-associated cytokine expression IFN-β. This pattern indicates a shift toward TRIF-dependent signaling with MPLA, reflecting a more anti-inflammatory or immunoregulatory profile. In the context of NEC, this is highly relevant: MyD88 signaling has been associated with epithelial barrier disruption and excessive inflammation, whereas TRIF signaling is thought to promote more controlled immune responses (29, 78-80). A TRIF-biased response, as induced by MPLA, may therefore be beneficial for preserving tight junction integrity and mitigating excessive inflammation.

4.6 Technical limitations

Consistency posed a significant challenge throughout this study, particularly in the Western blot analyses, which proved difficult to reproduce. Rather than quantifying protein concentration of each sample, we assumed equal protein content and loaded equal volumes, normalizing the results by β-actin. While β-actin expression was relatively stable across blots and samples, protein levels of Occludin and ZO-1 showed considerable variability. The underlying cause of this variability remains unclear, but must be addressed in future experiments to draw reliable conclusions regarding tight junction integrity. Only once this issue is resolved, MPLA and DPLA can be used with confidence to investigate how LPS dephosphorylation impacts tight junctions.

Another important consideration concerns the LPS concentrations used. Literature reports a wide range of LPS dosages, with many studies using concentrations as high as 100µg/ml(67, 68, 75), whereas clinically relevant levels are estimated to lie between 1-10ng/ml (35). We deliberately opted to work with lower concentrations where possible. However, intestinal epithelial cells such as CaCo2 and IEC6 appear less responsive to LPS than macrophages. In our TLR4 signaling experiments using RAW 264.7 cells, we used 100ng/ml, a relatively high dose for clinical significance, but appropriate for pathway activation analysis. Nevertheless, future studies should

include a broader range of clinically relevant LPS concentrations to better mimic physiological conditions.

Our qPCR analysis also had several limitations. Relative gene expression was calculated based on absolute quantities derived from standard curves. In an early experiment, only 1-hour samples were used, and the standard curve was constructed solely from these samples. Consequently, the resulting quantities may not be directly comparable to experiments where both 1 hour and 18 hour samples were included in the standard curve. This variation may have affected the reliability of fold-change calculations and, consequently, the statistical significance. Amplification efficiency was another concern. Initial experiments showed acceptable efficiency (90-110%), but in later experiments, this occasionally dropped to 70-100%. In particular, IFNβ showed poor efficiency, likely due to low expression levels or limited sensitivity of the primers used. The reasons for reduced efficiency in other targets remain unclear, but may involve RNA quality, pipetting inconsistencies during standard curve preparation, or gradual changes in primer concentration over time due to repeated freeze-thaw cycles. Despite these issues, relative expression levels between samples remained comparable, allowing for meaningful interpretation of gene expression differences.

Finally, due to the exploratory nature of this study and time constraints, not all experiments were performed in biological triplicate. Therefore, achieving statistical significance posed an issue. Future work should focus on repeating key experiments in triplicate to confirm data reliability and reproducibility.

4.7 Future perspectives

Although we were unable to clearly demonstrate a relationship between LPS, DPLA, or MPLA and tight junction disruption, our findings indicate that MPLA induces a more TRIF-dependent TLR4 signaling profile compared to DPLA and LPS. This suggests that dephosphorylated LPS is less pro-inflammatory and may even exert protective effects. This finding supports the relevance of alkaline phosphatase, which is known to dephosphorylate and thought to detoxify LPS (61). Notably, breast milk, which contains alkaline phosphatase, is widely recognized as the most effective means of preventing NEC (50-56). Its protective effect may therefore be mediated, at least in part, by the dephosphorylation of LPS through the action of alkaline phosphatase. Even though our study does not directly show the role of alkaline phosphatase in preserving tight junction integrity, we do observe a shift from MyD88- to TRIF-dependent signaling with MPLA treatment. Given the association between MyD88 signaling and tight junction disruption (78), it is plausible that this signaling shift contributes to the preservation of epithelial barrier function. Thus, by promoting TRIF-biased signaling, alkaline phosphatase may indirectly protect against epithelial barrier dysfunction.

One important challenge is that preterm infants are often unable to receive maternal breast milk due to factors such as difficulty with latching or suckling, as well as maternal illness or insufficient milk supply (81-83). As a result, they may lack exposure to protective components like alkaline phosphatase, which could contribute to their heightened vulnerability to NEC. Therefore, supplementing infant formula or clinical treatments with alkaline phosphatase, a natural and established component of breast milk, could represent a promising strategy to reduce NEC incidence.

To explore this possibility, future studies should aim to develop a robust and reproducible model of tight junction disruption in intestinal epithelial cells. This would enable direct evaluation of the protective effects of LPS dephosphorylation. In addition, experiments can also focus on other ways of measuring the epithelial barrier function. For example, a transepithelial electrical resistance (TEER) assay can provide quantitative insights into changes in epithelial integrity by measuring electrical resistance across the cell monolayer. Since the LPS concentrations used in our study were relatively high, incorporating clinically relevant concentrations of LPS will enhance the translation value of the findings. Our analysis was limited to gene expression of cytokines, and therefore only products of the MyD88- and TRIF-dependent pathway. A broader investigation into the specific pathway activation would strengthen our understanding of TLR4 signaling and its impact on diseases such as NEC. Finally, future experiments should directly assess the protective effects of alkaline phosphatase. This could be achieved by pre-incubating cells with alkaline phosphatase prior to LPS treatment, and comparing the outcomes to cells exposed to LPS alone. Ultimately, these future perspectives could pave the way for strategies to protect against diseases such as NEC.

5. Conclusion

This study set out to investigate whether MPLA, a dephosphorylated form of LPS, reduces tight junction disruption and promotes TRIF-dependent over MyD88-dependent TLR4 signaling compared to DPLA and LPS. While we did not observe consistent changes in tight junction proteins in intestinal epithelial cells, our findings indicate that MPLA induces a more TRIF-biased signaling profile, characterized by reduced expression of MyD88-associated cytokines (TNF-α, IL-1β) and relatively higher induction of TRIF-associated IFN-β. These results suggest that LPS dephosphorylation may attenuate pro-inflammatory signaling and potentially contribute to epithelial barrier integrity. This result highlights the potential of LPS dephosphorylation by enzymes such as alkaline phosphatase as a therapeutic strategy to prevent NEC.

6. Bibliography

1. Jones, I. H., & Hall, N. J. (2020). Contemporary Outcomes for Infants with Necrotizing Enterocolitis-A Systematic Review. *The Journal of pediatrics*, *220*, 86–92.e3. https://doi.org/10.1016/j.jpeds.2019.11.011
2. Bazacliu, C., & Neu, J. (2019). Necrotizing Enterocolitis: Long Term Complications. *Current pediatric reviews*, *15*(2), 115–124. https://doi.org/10.2174/1573396315666190312093119
3. Schulzke, S. M., Deshpande, G. C., & Patole, S. K. (2007). Neurodevelopmental outcomes of very low-birth-weight infants with necrotizing enterocolitis: a systematic review of observational studies. *Archives of pediatrics & adolescent medicine*, *161*(6), 583–590. https://doi.org/10.1001/archpedi.161.6.583
4. Samuels, N., van de Graaf, R. A., de Jonge, R. C. J., Reiss, I. K. M., & Vermeulen, M. J. (2017). Risk factors for necrotizing enterocolitis in neonates: a systematic review of prognostic studies. *BMC pediatrics*, *17*(1), 105. https://doi.org/10.1186/s12887-017-0847-3
5. Neu, J., & Walker, W. A. (2011). Necrotizing enterocolitis. *The New England journal of medicine*, *364*(3), 255–264. https://doi.org/10.1056/NEJMra1005408
6. Tanner, S. M., Berryhill, T. F., Ellenburg, J. L., Jilling, T., Cleveland, D. S., Lorenz, R. G., & Martin, C. A. (2015). Pathogenesis of necrotizing enterocolitis: modeling the innate immune response. *The American journal of pathology*, *185*(1), 4–16. https://doi.org/10.1016/j.ajpath.2014.08.028
7. Hunter, C. J., Upperman, J. S., Ford, H. R., & Camerini, V. (2008). Understanding the susceptibility of the premature infant to necrotizing enterocolitis (NEC). *Pediatric research*, *63*(2), 117–123. https://doi.org/10.1203/PDR.0b013e31815ed64c
8. Niño, D. F., Sodhi, C. P., & Hackam, D. J. (2016). Necrotizing enterocolitis: new insights into pathogenesis and mechanisms. *Nature reviews. Gastroenterology & hepatology*, *13*(10), 590–600. https://doi.org/10.1038/nrgastro.2016.119
9. Poltorak, A., He, X., Smirnova, I., Liu, M. Y., Van Huffel, C., Du, X., Birdwell, D., Alejos, E., Silva, M., Galanos, C., Freudenberg, M., Ricciardi-Castagnoli, P., Layton, B., & Beutler, B. (1998). Defective LPS signaling in C3H/HeJ and C57BL/10ScCr mice: mutations in Tlr4 gene. *Science (New York, N.Y.)*, *282*(5396), 2085–2088. https://doi.org/10.1126/science.282.5396.2085
10. Beveridge T. J. (1999). Structures of gram-negative cell walls and their derived membrane vesicles. *Journal of bacteriology*, *181*(16), 4725–4733. https://doi.org/10.1128/JB.181.16.4725-4733.1999
11. Park, B. S., Song, D. H., Kim, H. M., Choi, B. S., Lee, H., & Lee, J. O. (2009). The structural basis of lipopolysaccharide recognition by the TLR4-MD-2 complex. *Nature*, *458*(7242), 1191–1195. https://doi.org/10.1038/nature07830
12. Raetz, C. R., & Whitfield, C. (2002). Lipopolysaccharide endotoxins. *Annual review of biochemistry*, *71*, 635–700. https://doi.org/10.1146/annurev.biochem.71.110601.135414
13. Dardelle, F., Phelip, C., Darabi, M., Kondakova, T., Warnet, X., Combret, E., Juranville, E., Novikov, A., Kerzerho, J., & Caroff, M. (2024). Diversity, Complexity, and Specificity of Bacterial Lipopolysaccharide (LPS) Structures Impacting Their Detection and Quantification. *International journal of molecular sciences*, *25*(7), 3927. https://doi.org/10.3390/ijms25073927
14. Kim, S. J., & Kim, H. M. (2017). Dynamic lipopolysaccharide transfer cascade to TLR4/MD2 complex via LBP and CD14. *BMB reports*, *50*(2), 55–57. https://doi.org/10.5483/bmbrep.2017.50.2.011
15. Kim, H. M., Park, B. S., Kim, J. I., Kim, S. E., Lee, J., Oh, S. C., Enkhbayar, P., Matsushima, N., Lee, H., Yoo, O. J., & Lee, J. O. (2007). Crystal structure of the TLR4-MD-2 complex with bound endotoxin antagonist Eritoran. *Cell*, *130*(5), 906–917. https://doi.org/10.1016/j.cell.2007.08.002
16. Neal, M. D., Leaphart, C., Levy, R., Prince, J., Billiar, T. R., Watkins, S., Li, J., Cetin, S., Ford, H., Schreiber, A., & Hackam, D. J. (2006). Enterocyte TLR4 mediates phagocytosis and translocation of bacteria across the intestinal barrier. *Journal of immunology (Baltimore, Md. : 1950)*, *176*(5), 3070–3079. https://doi.org/10.4049/jimmunol.176.5.3070
17. Medzhitov, R., Preston-Hurlburt, P., Kopp, E., Stadlen, A., Chen, C., Ghosh, S., & Janeway, C. A., Jr (1998). MyD88 is an adaptor protein in the hToll/IL-1 receptor family signaling pathways. *Molecular cell*, *2*(2), 253–258. https://doi.org/10.1016/s1097-2765(00)80136-7
18. Davis, C. N., Mann, E., Behrens, M. M., Gaidarova, S., Rebek, M., Rebek, J., Jr, & Bartfai, T. (2006). MyD88-dependent and -independent signaling by IL-1 in neurons probed by bifunctional Toll/IL-1 receptor domain/BB-loop mimetics. *Proceedings of the National Academy of Sciences of the United States of America*, *103*(8), 2953–2958. https://doi.org/10.1073/pnas.0510802103
19. Kenny, E. F., & O'Neill, L. A. (2008). signaling adaptors used by Toll-like receptors: an update. *Cytokine*, *43*(3), 342–349. https://doi.org/10.1016/j.cyto.2008.07.010
20. Horng, T., Barton, G. M., Flavell, R. A., & Medzhitov, R. (2002). The adaptor molecule TIRAP provides signaling specificity for Toll-like receptors. *Nature*, *420*(6913), 329–333. https://doi.org/10.1038/nature01180
21. Yamamoto, M., Sato, S., Hemmi, H., Sanjo, H., Uematsu, S., Kaisho, T., Hoshino, K., Takeuchi, O., Kobayashi, M., Fujita, T., Takeda, K., & Akira, S. (2002). Essential role for TIRAP in activation of the signaling cascade shared by TLR2 and TLR4. *Nature*, *420*(6913), 324–329. https://doi.org/10.1038/nature01182

22. Yamamoto, M., Sato, S., Hemmi, H., Hoshino, K., Kaisho, T., Sanjo, H., Takeuchi, O., Sugiyama, M., Okabe, M., Takeda, K., & Akira, S. (2003). Role of adaptor TRIF in the MyD88-independent toll-like receptor signaling pathway. *Science (New York, N.Y.)*, *301*(5633), 640–643. https://doi.org/10.1126/science.1087262
23. Yamamoto, M., Sato, S., Hemmi, H., Uematsu, S., Hoshino, K., Kaisho, T., Takeuchi, O., Takeda, K., & Akira, S. (2003). TRAM is specifically involved in the Toll-like receptor 4-mediated MyD88-independent signaling pathway. *Nature immunology*, *4*(11), 1144–1150. https://doi.org/10.1038/ni986
24. Li, J., Lee, D. S., & Madrenas, J. (2013). Evolving Bacterial Envelopes and Plasticity of TLR2-Dependent Responses: Basic Research and Translational Opportunities. *Frontiers in immunology*, *4*, 347. https://doi.org/10.3389/fimmu.2013.00347
25. Cheng, Z., Taylor, B., Ourthiague, D. R., & Hoffmann, A. (2015). Distinct single-cell signaling characteristics are conferred by the MyD88 and TRIF pathways during TLR4 activation. *Science signaling*, *8*(385), ra69. https://doi.org/10.1126/scisignal.aaa5208
26. Planès, R., Ben Haij, N., Leghmari, K., Serrero, M., BenMohamed, L., & Bahraoui, E. (2016). HIV-1 Tat Protein Activates both the MyD88 and TRIF Pathways To Induce Tumor Necrosis Factor Alpha and Interleukin-10 in Human Monocytes. *Journal of virology*, *90*(13), 5886–5898. https://doi.org/10.1128/JVI.00262-16
27. Brieger, A., Rink, L., & Haase, H. (2013). Differential regulation of TLR-dependent MyD88 and TRIF signaling pathways by free zinc ions. *Journal of immunology (Baltimore, Md. : 1950)*, *191*(4), 1808–1817. https://doi.org/10.4049/jimmunol.1301261
28. Kawasaki, T., & Kawai, T. (2014). Toll-like receptor signaling pathways. *Frontiers in immunology*, *5*, 461. https://doi.org/10.3389/fimmu.2014.00461
29. Yang, G., Bao, P., Zhang, L., Lyu, Z., Zhou, B., Chen, K., Peng, S., Wang, Y., Yao, L., Zhou, Y., & Li, Y. (2014). Critical role of myeloid differentiation factor 88 in necrotizing enterocolitis. *Pediatric research*, *75*(6), 707–715. https://doi.org/10.1038/pr.2014.39
30. Shen, L., & Turner, J. R. (2006). Role of epithelial cells in initiation and propagation of intestinal inflammation. Eliminating the static: tight junction dynamics exposed. *American journal of physiology. Gastrointestinal and liver physiology*, *290*(4), G577–G582. https://doi.org/10.1152/ajpgi.00439.2005
31. Godbole, N. M., Chowdhury, A. A., Chataut, N., & Awasthi, S. (2022). Tight Junctions, the Epithelial Barrier, and Toll-like Receptor-4 During Lung Injury. *Inflammation*, *45*(6), 2142–2162. https://doi.org/10.1007/s10753-022-01708-y
32. Lee, B., Moon, K. M., & Kim, C. Y. (2018). Tight Junction in the Intestinal Epithelium: Its Association with Diseases and Regulation by Phytochemicals. *Journal of immunology research*, *2018*, 2645465. https://doi.org/10.1155/2018/2645465
33. Kuo, W. T., Odenwald, M. A., Turner, J. R., & Zuo, L. (2022). Tight junction proteins occludin and ZO-1 as regulators of epithelial proliferation and survival. *Annals of the New York Academy of Sciences*, *1514*(1), 21–33. https://doi.org/10.1111/nyas.14798
34. Guo, S., Nighot, M., Al-Sadi, R., Alhmoud, T., Nighot, P., & Ma, T. Y. (2015). Lipopolysaccharide Regulation of Intestinal Tight Junction Permeability Is Mediated by TLR4 Signal Transduction Pathway Activation of FAK and MyD88. *Journal of immunology (Baltimore, Md. : 1950)*, *195*(10), 4999–5010. https://doi.org/10.4049/jimmunol.1402598
35. Guo, S., Al-Sadi, R., Said, H. M., & Ma, T. Y. (2013). Lipopolysaccharide causes an increase in intestinal tight junction permeability in vitro and in vivo by inducing enterocyte membrane expression and localization of TLR-4 and CD14. *The American journal of pathology*, *182*(2), 375–387. https://doi.org/10.1016/j.ajpath.2012.10.014
36. Sheth, P., Delos Santos, N., Seth, A., LaRusso, N. F., & Rao, R. K. (2007). Lipopolysaccharide disrupts tight junctions in cholangiocyte monolayers by a c-Src-, TLR4-, and LBP-dependent mechanism. *American journal of physiology. Gastrointestinal and liver physiology*, *293*(1), G308–G318. https://doi.org/10.1152/ajpgi.00582.2006
37. Leaphart, C. L., Cavallo, J., Gribar, S. C., Cetin, S., Li, J., Branca, M. F., Dubowski, T. D., Sodhi, C. P., & Hackam, D. J. (2007). A critical role for TLR4 in the pathogenesis of necrotizing enterocolitis by modulating intestinal injury and repair. *Journal of immunology (Baltimore, Md. : 1950)*, *179*(7), 4808–4820. https://doi.org/10.4049/jimmunol.179.7.4808
38. Ahle, M., Drott, P., Elfvin, A., & Andersson, R. E. (2018). Maternal, fetal and perinatal factors associated with necrotizing enterocolitis in Sweden. A national case-control study. *PloS one*, *13*(3), e0194352. https://doi.org/10.1371/journal.pone.0194352
39. Sharma, R., & Hudak, M. L. (2013). A clinical perspective of necrotizing enterocolitis: past, present, and future. *Clinics in perinatology*, *40*(1), 27–51. https://doi.org/10.1016/j.clp.2012.12.012
40. Fusunyan, R. D., Nanthakumar, N. N., Baldeon, M. E., & Walker, W. A. (2001). Evidence for an innate immune response in the immature human intestine: toll-like receptors on fetal enterocytes. *Pediatric research*, *49*(4), 589–593. https://doi.org/10.1203/00006450-200104000-00023
41. Neal, M. D., Sodhi, C. P., Dyer, M., Craig, B. T., Good, M., Jia, H., Yazji, I., Afrazi, A., Richardson, W. M., Beer-Stolz, D., Ma, C., Prindle, T., Grant, Z., Branca, M. F., Ozolek, J., & Hackam, D. J. (2013). A critical role for TLR4 induction

of autophagy in the regulation of enterocyte migration and the pathogenesis of necrotizing enterocolitis. *Journal of immunology (Baltimore, Md. : 1950)*, *190*(7), 3541–3551. https://doi.org/10.4049/jimmunol.1202264

42. Nanthakumar, N., Meng, D., Goldstein, A. M., Zhu, W., Lu, L., Uauy, R., Llanos, A., Claud, E. C., & Walker, W. A. (2011). The mechanism of excessive intestinal inflammation in necrotizing enterocolitis: an immature innate immune response. *PloS one*, *6*(3), e17776. https://doi.org/10.1371/journal.pone.0017776
43. Parkin, K., Christophersen, C. T., Verhasselt, V., Cooper, M. N., & Martino, D. (2021). Risk Factors for Gut Dysbiosis in Early Life. *Microorganisms*, *9*(10), 2066. https://doi.org/10.3390/microorganisms9102066
44. Cuna, A., Morowitz, M. J., Ahmed, I., Umar, S., & Sampath, V. (2021). Dynamics of the preterm gut microbiome in health and disease. *American journal of physiology. Gastrointestinal and liver physiology*, *320*(4), G411–G419
45. Fundora, J. B., Guha, P., Shores, D. R., Pammi, M., & Maheshwari, A. (2020). Intestinal dysbiosis and necrotizing enterocolitis: assessment for causality using Bradford Hill criteria. *Pediatric research*, *87*(2), 235–248. https://doi.org/10.1038/s41390-019-0482-9
46. Salguero, M. V., Al-Obaide, M. A. I., Singh, R., Siepmann, T., & Vasylyeva, T. L. (2019). Dysbiosis of Gram-negative gut microbiota and the associated serum lipopolysaccharide exacerbates inflammation in type 2 diabetic patients with chronic kidney disease. *Experimental and therapeutic medicine*, *18*(5), 3461–3469. https://doi.org/10.3892/etm.2019.7943
47. D., Stoll, B. J., & Eunice Kennedy Shriver National Institute of Child Health and Human Development Neonatal Research Network (2015). Causes and timing of death in extremely premature infants from 2000 through 2011. *The New England journal of medicine*, *372*(4), 331–340. https://doi.org/10.1056/NEJMoa1403489
48. Wu, H., Guo, K., Zhuo, Z., Zeng, R., Luo, Y., Yang, Q., Li, J., Jiang, R., Huang, Z., Sha, W., & Chen, H. (2022). Current therapy option for necrotizing enterocolitis: Practicalities and challenge. *Frontiers in pediatrics*, *10*, 954735. https://doi.org/10.3389/fped.2022.954735
49. Hu, X., Liang, H., Li, F., Zhang, R., Zhu, Y., Zhu, X., & Xu, Y. (2024). Necrotizing enterocolitis: current understanding of the prevention and management. *Pediatric surgery international*, *40*(1), 32. https://doi.org/10.1007/s00383-023-05619-3
50. Guthrie, S. O., Gordon, P. V., Thomas, V., Thorp, J. A., Peabody, J., & Clark, R. H. (2003). Necrotizing enterocolitis among neonates in the United States. *Journal of perinatology : official journal of the California Perinatal Association*, *23*(4), 278–285. https://doi.org/10.1038/sj.jp.7210892
51. Alsaied, A., Islam, N., & Thalib, L. (2020). Global incidence of Necrotizing Enterocolitis: a systematic review and Meta-analysis. *BMC pediatrics*, *20*(1), 344. https://doi.org/10.1186/s12887-020-02231-5
52. Schanler, R. J., Shulman, R. J., & Lau, C. (1999). Feeding strategies for premature infants: beneficial outcomes of feeding fortified human milk versus preterm formula. *Pediatrics*, *103*(6 Pt 1), 1150–1157. https://doi.org/10.1542/peds.103.6.1150
53. Sullivan, S., Schanler, R. J., Kim, J. H., Patel, A. L., Trawöger, R., Kiechl-Kohlendorfer, U., Chan, G. M., Blanco, C. L., Abrams, S., Cotten, C. M., Laroia, N., Ehrenkranz, R. A., Dudell, G., Cristofalo, E. A., Meier, P., Lee, M. L., Rechtman, D. J., & Lucas, A. (2010). An exclusively human milk-based diet is associated with a lower rate of necrotizing enterocolitis than a diet of human milk and bovine milk-based products. *The Journal of pediatrics*, *156*(4), 562–7.e1. https://doi.org/10.1016/j.jpeds.2009.10.040
54. Cristofalo, E. A., Schanler, R. J., Blanco, C. L., Sullivan, S., Trawoeger, R., Kiechl-Kohlendorfer, U., Dudell, G., Rechtman, D. J., Lee, M. L., Lucas, A., & Abrams, S. (2013). Randomized trial of exclusive human milk versus preterm formula diets in extremely premature infants. *The Journal of pediatrics*, *163*(6), 1592–1595.e1. https://doi.org/10.1016/j.jpeds.2013.07.011
55. Quigley, M., Embleton, N. D., & McGuire, W. (2019). Formula versus donor breast milk for feeding preterm or low birth weight infants. *The Cochrane database of systematic reviews*, *7*(7), CD002971. https://doi.org/10.1002/14651858.CD002971.pub5
56. Altobelli, E., Angeletti, P. M., Verrotti, A., & Petrocelli, R. (2020). The Impact of Human Milk on Necrotizing Enterocolitis: A Systematic Review and Meta-Analysis. *Nutrients*, *12*(5), 1322. https://doi.org/10.3390/nu12051322
57. Li, B., Wu, R. Y., Horne, R. G., Ahmed, A., Lee, D., Robinson, S. C., Zhu, H., Lee, C., Cadete, M., Johnson-Henry, K. C., Landberg, E., Alganabi, M., Abrahamsson, T., Delgado-Olguin, P., Pierro, A., & Sherman, P. M. (2020). Human Milk Oligosaccharides Protect against Necrotizing Enterocolitis by Activating Intestinal Cell Differentiation. *Molecular nutrition & food research*, *64*(21), e2000519. https://doi.org/10.1002/mnfr.202000519
58. Gopalakrishna, K. P., Macadangdang, B. R., Rogers, M. B., Tometich, J. T., Firek, B. A., Baker, R., Ji, J., Burr, A. H. P., Ma, C., Good, M., Morowitz, M. J., & Hand, T. W. (2019). Maternal IgA protects against the development of necrotizing enterocolitis in preterm infants. *Nature medicine*, *25*(7), 1110–1115. https://doi.org/10.1038/s41591-019-0480-9
59. CHANDA, R., OWEN, E. C., & CRAMOND, B. (1951). The composition of human milk with special reference to the relation between phosphorus partition and phosphatase and to the partition of certain vitamins. *The British journal of nutrition*, *5*(2), 228–242. https://doi.org/10.1079/bjn19510029
60. STEWART, R. A., PLATOU, E., & KELLY, V. J. (1958). The alkaline phosphatase content of human milk. *The Journal of biological chemistry*, *232*(2), 777–784.
61. Poelstra, K., Bakker, W. W., Klok, P. A., Kamps, J. A., Hardonk, M. J., & Meijer, D. K. (1997). Dephosphorylation of endotoxin by alkaline phosphatase in vivo. *The American journal of pathology*, *151*(4), 1163–1169.

62. Gustafson, G. L., & Rhodes, M. J. (1992). A rationale for the prophylactic use of monophosphoryl lipid A in sepsis and septic shock. *Biochemical and biophysical research communications*, *182*(1), 269–275. https://doi.org/10.1016/s0006-291x(05)80140-8
63. Ruchaud-Sparagano, M. H., Mills, R., Scott, J., & Simpson, A. J. (2014). MPLA inhibits release of cytotoxic mediators from human neutrophils while preserving efficient bacterial killing. *Immunology and cell biology*, *92*(9), 799–809. https://doi.org/10.1038/icb.2014.55
64. Watts, B. A., 3rd, George, T., Sherwood, E. R., & Good, D. W. (2017). Monophosphoryl lipid A induces protection against LPS in medullary thick ascending limb through a TLR4-TRIF-PI3K signaling pathway. *American journal of physiology. Renal physiology*, *313*(1), F103–F115. https://doi.org/10.1152/ajprenal.00064.2017
65. Albert Vega, C., Karakike, E., Bartolo, F., Mouton, W., Cerrato, E., Brengel-Pesce, K., Giamarellos-Bourboulis, E. J., Mallet, F., & Trouillet-Assant, S. (2021). Differential response induced by LPS and MPLA in immunocompetent and septic individuals. *Clinical immunology (Orlando, Fla.)*, *226*, 108714. https://doi.org/10.1016/j.clim.2021.108714
66. Schippers, M., Post, E., Eichhorn, I., Langeland, J., Beljaars, L., Malo, M. S., Hodin, R. A., Millán, J. L., Popov, Y., Schuppan, D., & Poelstra, K. (2020). Phosphate Groups in the Lipid A Moiety Determine the Effects of LPS on Hepatic Stellate Cells: A Role for LPS-Dephosphorylating Activity in Liver Fibrosis. *Cells*, *9*(12), 2708. https://doi.org/10.3390/cells9122708
67. Yang, M., Xu, W., Yue, C., Li, R., Huang, X., Yan, Y., Yan, Q., Liu, S., Liu, Y., & Li, Q. (2025). Adipose-derived stem cells promote the recovery of intestinal barrier function by inhibiting the p38 MAPK signaling pathway. *European journal of histochemistry : EJH*, *69*(1), 4158. https://doi.org/10.4081/ejh.2025.4158
68. Fang, W., Zhao, P., Shen, A., Liu, L., Chen, H., Chen, Y., Peng, J., Sferra, T. J., Sankararaman, S., Luo, Y., & Ke, X. (2021). Effects of Qing Hua Chang Yin on lipopolysaccharide-induced intestinal epithelial tight junction injury in Caco-2 cells. *Molecular medicine reports*, *23*(3), 205. https://doi.org/10.3892/mmr.2021.11844
69. Chen, Y., Zhang, L., Zhang, Y., Bai, T., Song, J., Qian, W., & Hou, X. (2020). EphrinA1/EphA2 Promotes Epithelial Hyperpermeability Involving in Lipopolysaccharide-induced Intestinal Barrier Dysfunction. *Journal of neurogastroenterology and motility*, *26*(3), 397–409. https://doi.org/10.5056/jnm19095
70. Witthöft, T., Eckmann, L., Kim, J. M., & Kagnoff, M. F. (1998). Enteroinvasive bacteria directly activate expression of iNOS and NO production in human colon epithelial cells. *The American journal of physiology*, *275*(3), G564–G571. https://doi.org/10.1152/ajpgi.1998.275.3.G564
71. Serreli, G., Melis, M. P., Corona, G., & Deiana, M. (2019). Modulation of LPS-induced nitric oxide production in intestinal cells by hydroxytyrosol and tyrosol metabolites: Insight into the mechanism of action. Food and chemical toxicology : an international journal published for the British Industrial Biological Research Association, 125, 520–527. https://doi.org/10.1016/j.fct.2019.01.039
72. Whitaker, R. H., & Cook, J. G. (2021). Stress Relief Techniques: p38 MAPK Determines the Balance of Cell Cycle and Apoptosis Pathways. Biomolecules, 11(10), 1444. https://doi.org/10.3390/biom11101444
73. Zhang, H., Xiong, Z., He, Y., Su, H., & Jiao, Y. (2025). Cimifugin improves intestinal barrier dysfunction by upregulating SIRT1 to regulate the NRF2/HO-1 signaling pathway. Naunyn-Schmiedeberg's archives of pharmacology, 398(3), 2897–2908. https://doi.org/10.1007/s00210-024-03433-9
74. Lee, J. B., Zgair, A., Taha, D. A., Zang, X., Kagan, L., Kim, T. H., Kim, M. G., Yun, H. Y., Fischer, P. M., & Gershkovich, P. (2017). Quantitative analysis of lab-to-lab variability in Caco-2 permeability assays. European journal of pharmaceutics and biopharmaceutics : official journal of Arbeitsgemeinschaft fur Pharmazeutische Verfahrenstechnik e.V, 114, 38–42. https://doi.org/10.1016/j.ejpb.2016.12.027
75. Ferruzza, S., Rossi, C., Scarino, M. L., & Sambuy, Y. (2012). A protocol for differentiation of human intestinal Caco-2 cells in asymmetric serum-containing medium. Toxicology in vitro : an international journal published in association with BIBRA, 26(8), 1252–1255. https://doi.org/10.1016/j.tiv.2012.01.008
76. Cummins P. M. (2012). Occludin: one protein, many forms. Molecular and cellular biology, 32(2), 242–250. https://doi.org/10.1128/MCB.06029-11
77. Mankertz, J., Waller, J. S., Hillenbrand, B., Tavalali, S., Florian, P., Schöneberg, T., Fromm, M., & Schulzke, J. D. (2002). Gene expression of the tight junction protein occludin includes differential splicing and alternative promoter usage. Biochemical and biophysical research communications, 298(5), 657–666. https://doi.org/10.1016/s0006-291x(02)02487-7
78. Nighot, M., Al-Sadi, R., Guo, S., Rawat, M., Nighot, P., Watterson, M. D., & Ma, T. Y. (2017). Lipopolysaccharide-Induced Increase in Intestinal Epithelial Tight Permeability Is Mediated by Toll-Like Receptor 4/Myeloid Differentiation Primary Response 88 (MyD88) Activation of Myosin Light Chain Kinase Expression. The American journal of pathology, 187(12), 2698–2710. https://doi.org/10.1016/j.ajpath.2017.08.005

79. Stockinger, S., Duerr, C. U., Fulde, M., Dolowschiak, T., Pott, J., Yang, I., Eibach, D., Bäckhed, F., Akira, S., Suerbaum, S., Brugman, M., & Hornef, M. W. (2014). TRIF signaling drives homeostatic intestinal epithelial antimicrobial peptide expression. Journal of immunology (Baltimore, Md. : 1950), 193(8), 4223–4234. https://doi.org/10.4049/jimmunol.1302708
80. Buchholz, B. M., Billiar, T. R., & Bauer, A. J. (2010). Dominant role of the MyD88-dependent signaling pathway in mediating early endotoxin-induced murine ileus. American journal of physiology. Gastrointestinal and liver physiology, 299(2), G531–G538. https://doi.org/10.1152/ajpgi.00060.2010
81. Breastfeeding Challenges: ACOG Committee Opinion, Number 820. (2021). Obstetrics and gynecology, 137(2), e42–e53. https://doi.org/10.1097/AOG.0000000000004253
82. Chen, L., Shang, Y., Tian, X., Huang, Y., Sun, Y., Fu, C., Bai, J., & Liu, Y. (2025). The struggles of breastfeeding mothers of preterm infants: a qualitative study. BMC pregnancy and childbirth, 25(1), 472. https://doi.org/10.1186/s12884-025-07597-x
83. Skaaning, D., Brødsgaard, A., Kronborg, H., Kyhnæb, A., Pryds, O., & Carlsen, E. (2024). Maternal Reasons for Early Termination of Exclusive Breastfeeding in Premature Infants: A Prospective Study. The Journal of perinatal & neonatal nursing, 38(1), 88–97. https://doi.org/10.1097/JPN.0000000000000693 Chu, C., Ru, H., Chen, Y., Xu, J., Wang, C., & Jin, Y. (2024). Gallic acid attenuates LPS-induced inflammation in Caco-2 cells by suppressing the activation of the NF-κB/MAPK signaling pathway. *Acta biochimica et biophysica Sinica*, *56*(6), 905–915. https://doi.org/10.3724/abbs.2024008

7. Appendices

MTT and NO assay

Materials:

General:

- 96 well plates
- Culture medium
- PBS
- Treatment solution
- DMSO

NO assay:

- 100 mM NaNO2 stock solution
- 1,5 ml tubes for the standard curve
- Griess solutions:
    - Griess A: 2gr Sulfanilamide en 5 ml phosphoric acid in total volume of 100ml MilliQ water
    - Griess B: 200mg N-(1-Naphthyl)ethylenediamine dihydrochloride in 100 ml MilliQ water

MTT assay:

- Tetrazolium

MTT and NO assay broad protocol

1. Seed cells in a 96-well flat bottom culture plate with cell medium in triplo if possible.
2. After 24h, remove the supernatant. Add 200µl/well fresh medium containing the following treatment.
3. After treatment incubation time, observe by microscope and collect 100 µl supernatant for NO assay. Now continue with the NO assay and MTT assay.

NO assay

Standard curve of sodium nitrite ($NaNO_2$)

1. Prepare stock-solution: 100mM $NaNo_2$-solution in MQ (0.69g/100ml)
2. Dilute stock-solution 100x in culture medium (= 1 mM solution), thus pipette 10ul 100mM $NaNO_2$ in 1 ml medium -> 1mM $NaNo_2$
3. Make the standard curve:

[NaNO2] (uM)	**V NaNO2**	**V medium**
100	100 ul 1 mM	900 ul
50	500 ul 100 uM	500 ul
25	500 ul 50 uM	500 ul
12.5	500 ul 25 uM	500 ul
6.3	500 ul 12,5 uM	500 ul
3.1	500 ul 6.3 uM	500 ul
1.6	500 ul 3,1 uM	500 ul
0.8	500 ul 1,6 uM	500 ul
0	-	500 ul

The NO reaction:

1. Pipette 100 ul of the standard curve samples in triplo in a 96 well plate
2. Pipette 100 ul of your experimental samples in empty wells
3. Make fresh Griess reagent by mixing equal volume of Griess A and Griess B
4. Pipette 100 ul of this fresh prepared Griess to all the standards and samples
5. Remove the bubbles out of the wells (they disturb the readout)
6. Measure the plate at 550 nM

MTT Assay Protocol

1. Prepare Tetrazolium (Sigma M5655; door VMT1 4°C) 0,5 mg/ml in your medium
2. Remove Medium from cells + soak of the supernatant carefully with a pipet with PBS + Remove PBS
3. Add 200 µl MTT-solution (0.5 mg/ml in DMEM) and incubate for an hour. Check under the mic! Remove MTT-solution very carefully from the wells with a pipet. Draw up from the corners of the well
4. Add 100 ul DMSO to each well and place on a shaker till the purple precipitate dissolves. (~10 minutes)
5. Measure the absorbance at 550 nm.

Protein isolation with RIPA buffer

Materials

50ml RIPA buffer:

- 500µl Igepal
- 250mg deoxycholic acid (sodium salt)
- 2.5ml 20% SDS
- Fill to 50ml with PBS

<u>Just before use add:</u>

40µl protease inhibitor cocktail per ml

To detect Phosphorylated proteins add:

- 10µl sodium orthovanadate (100 mM) per ml
- 10µl NaF (1M) per ml
- 50µl 20x phosphostop per ml

Without protease cocktail, RIPA buffer can be stored for a long time at 4 degrees

Method:

Cell culture:

1. Wash cells twice with pre chilled PBS
2. Add 125µl RIPA on cell culture in 6 well (add more if necessary)
3. Shear DNA with an insulin needle (5x forced through needle)
4. Add 40µl loading buffer (LB4X)
5. Boil the sample for 5 minutes

6. Bring 10-15µl of samples on the SDS-PAGE gel.
7. Rest of the sample can be stored at -20 degrees.
8. After thawing, reboil samples for 1-2 minutes before use.

Western blot

Ingredients:
SDS page gel 1.5mm

Separating gel	7.5% Acrylamide	10% Acrylamide
H2O	8.205ml	7.75ml
1,5M Tris-HCL pH 8.8	3.75ml	4ml
10% (v/w) SDS	150µl	160µl
Acrylamide/bis	2.82ml	4ml
10% APS	75µl	80µl
TEMED	23µl	24µl

Stacking gel	7.5% Acrylamide	10% Acrylamide
H2O	6.3ml	3.78ml
1,5M Tris-HCL pH 8.8	2.5ml	1.5ml
10% (v/w) SDS	100µl	60µl
Acrylamide/bis	1ml	1.2ml
10% APS	50µl	30µl
TEMED	15µl	9µl
Broomphenolblue	10µl	10µl

Electrophoresis buffer: 1L = 15,1g Tris base, 94g Glycine, 50ml 10% SDS, fill to 1L with water.
Blot buffer = 1L = 3,03g Tris base, 14,4g Glycine, 200ml methanol, fill to 1L with water.
TBST = 1L = 8g NaCl, 0.2g KCl, 1.44g Na_2HPO_4, 0.24g KH_2PO_4, 1ml Tween-20, fill to 1L with water.

Create a gel:

Pour a PAA geld with an acrylamide concentration that fits your need to separate proteins with different sizes. (Lower concentration might be better for higher molecular weight markers)

1. Create a glass plate construction in which your gel can be made.
2. Prepare a separation gel according to the table. Straight after adding TEMED and APS to the solution, mix it and pour the solution between the glass plate construction until 2cm beneath the top of the smallest glass plate.
3. Add about 1ml 2-butanol on top of the separation gel to create an airtight and straight topline of the gel.
4. Let the solution polymerise for about 30 minutes
5. When the gel is solid, take off the butanol and wash off the butanol with H2O. Remove all water left.
6. Prepare a stack gel solution according to the table. Again after adding TEMED and APS, mix and pour the stacking solution on top of the separation gel filling the glass plate.
7. Take a comb with the correct depth and place it in the stack.
8. Let the solution polymerize for about 30 minutes

Preparing the electrophoresis system:

1. Choose the precise protein gel needed for your job
2. Create the electrophoresis system by filling the inner chamber with an electrophoresis buffer until it is halfway between the tops of the taller and shorter glass plates of the gel cassettes. Fill the outer chamber with ~200ml electrophoresis buffer.
3. Load samples into the wells.
4. Run the system: 50v for 5 minutes (until the samples reach the separation layer), then 100v for 90-120 minutes (depending on the size of the protein).

Gel removal

1. After electrophoresis is complete, turn off the power supply and disconnect the electrical leads.
2. Remove the tank lid and pour out the buffer.
3. Gently lift out the inner chamber assembly.
4. Remove the gels from the gel cassette by gently separating the two plates of the gel cassette. The green, wedge shaped, plastic Gel releaser may be used to help pry the glass plates apart.
5. Remove the wells part of the gel.

Blotting

1. Prepare the gel sandwich. Always wear gloves when handling membranes.
    a. Place the cassette, with the black side down in a box with a blotting buffer.
    b. Place one pre-wetted fiber pad on the black side on the cassette.
    c. Place a sheet of filter paper on the fiber pad.
    d. Place the gel on the filter paper
    e. Place the pre-wetted nitrocellulose membrane on the gel
    f. Complete the sandwich by placing a piece of paper on the membrane and add the last fiber pad.
    g. Remove all air bubbles, by rolling with a roller over the sandwich.

2. Close the cassette and place the cassette in the holder. (black to black, white facing red)
3. Add a frozen cooling unit in the holder and fill the tank with a blotting buffer.
4. Put the holder in a box with ice.
5. Run the system: 100v for 90 minutes.
6. After blotting is completed remove the membrane, and add Ponceau to see if proteins are on the membrane.
7. Pour the ponceau back into the flask and wash the membrane with H2O until water is no longer very red.

Blocking and incubation with antibodies

1. Block the membrane for 120 minutes with 5% skimmed milk
2. Wash 3 times for 2 minutes with TBST
3. Dilute the primary antibody in 5ml TBST
4. Incubate primary antibody by putting it on a rollerbank (3 hours room temperature or overnight in the cold room)
5. Wash 3 times for 2 minutes with TBST
6. Dilute the secondary antibody in 5ml blocking solution
7. Incubate the secondary antibody by putting it on a rollerbank (2 hours room temperature or overnight in the cold room)
8. Wash the membranes 3 times for 2 minutes with TBST

Visualization

1. Mix supersignal 1 and supersignal 2 1:1, Pour the SS mixture over the whole membrane.
2. Put the membrane on a plastic slide on the drawer into the uvitec.
3. Make a chemiluminescent picture on auto mode.
4. Change settings if needed.
5. Quantify using the uvitec software.
6. To save the membrane wash with TBST and store in TBST.

Confocal microscopy CaCo2 and IEC6

Materials:

- Fixation: 4% formaldehyde
- Permeabilization: 1mg/ml saponin
- Nucleus staining solution: Hoechst 33342 stock = 10ug/ml -> freezer 1µl per ml.
- Primary antibody: 5µl in 300µl pbs, put 50 µl on cells.
- Secondary antibody: 5µl in 300µl pbs, put 50 µl on cells.
- blocking solution, 3% bsa, in fridge 30mg/ml
- DPBS

Day 1: Seed cells in a 96 well plate, incubate for 24h
Day 2: Treat cells with 10 - 10.000 ng/ml lps for 24/48h
Day 3/4: After 24/48h, remove the medium and use PBS to wash 2 times

1. **Fixation:** Add 100 µL fixation solution and incubate at room temperature for 20 minutes.

2. **Permeabilization:** Remove the fixation solution and wash 3 times with 100 µL DPBS. Add 100 µL of permeabilization solution for 5 min RT.
3. **Blocking:** remove the permeabilization solution and carefully wash 3 times with 100 µL DPBS. Add 100 µL blocking solution and incubate for 60 minutes at room temperature.
4. **Primary antibody:** Remove the blocking solution, wash 3 times, add 50µL primary antibody, and incubate in the dark for 30-60 minutes at room temperature.
5. **Secondary antibody:** Remove the primary antibody solution and wash 3 times with DPBS. Add 50µL secondary antibody solution, and incubate in the dark for 30-60 minutes at room temperature.
6. **Nucleus staining:** Remove the secondary antibody solution and wash 3 times with DPBS. Add nucleus staining solution* and incubate in the dark for 5 minutes at room temperature.
7. **Imaging**: Remove the nucleus staining solution and wash 3 times with DPBS. The sample is ready for fluorescent imaging.

Total time = 4.5 hours

Use an only secondary antibody as well to check background fluorescence.

Flow cytometry protocol TLR4

Materials:

EDTA/Lidocaine solution for detachment

- 10mM EDTA (#406)
- 4,4 mg/ml lidocaine (#56)
- 10% FBS (add just before use)

Staining buffer

- dPBS
- 2% FBS
- 5mM EDTA

Antibodies:

anti-TLR4, rabbit polyclonal (ab13556)

Alexafluor 488 anti rabbit (A-11008)

Controls:

- Negative control (NC): Unstained cells. Don't add antibodies, add clean staining buffer instead of antibodies.
- Background staining control (Bc): Only 2nd antibody, to check if your secondary antibody has background staining. Don't add 1st antibody
- Positive control: Cells that for sure express your protein of interest. In the case of TLR4 RAW cells. This positive control should have a negative control and background staining control as well.

Protocol:

Day 1: cell seeding

1. Seed cells in a 12-well plate, at a density of 4*10^4 cells/cm2
2. Grow them at 37C overnight

Day 2: stimulation/polarisation

1. Depending on cells and research question, stimulate or polarize cells
2. Continue growing them at 37C

Day3: staining

Cell detachment

1. Check cell status under microscope, happy or dead?
2. Discard the medium and was cells twice with dPBS
3. Add 0,5ml of EDTA/Lidocaine solution to each well. Incubate for ~5 minutes at 37C. Check if cells are detached in-between. Incubate for longer if needed.
4. Check if cells are happy under the microscope
5. Per well: Pipet the medium up and down firmly to detach the cells from the bottom of the plate. Collect the cells in a 2,5ml eppendorf
6. Centrifuge the cells for 4 minutes, 300g at room temperature.
7. Check your pellet, and discard the EDTA/lidocaine solution. Tap your cells loose (same as during cell culture) and add 2ml of the staining buffer

Cell staining

1. Count the cells, and seed 50.000cells per 200ul staining buffer in a round bottom 96-well plate
2. Centrifuge cells for 5 minutes, 300g, RT
3. Discard medium, wash by adding 200ul staining buffer, and pipet a few times up and down very gently (make sure pellet is dissolved)
4. Centrifuge cells for 5 minutes, 300g, RT, discard medium.
5. Stain with 25ul 1:100 diluted primary antibody per well, for 30 minutes at 4C. Resuspend cells gently in the primary antibody solution before incubation.
    - Negative control -1st and -2nd antibody
    - Background -1st antibody
6. Centrifuge cells for 5 minutes, 300g, RT, discard supernatant
7. Wash twice by adding 200ul staining buffer, centrifuging and discarding supernatant.
8. Stain with 25ul 1:250 secondary antibody per well, for 30 minutes at 4C in the dark. Resuspend the cells gently before incubation

From now on keep the cells as much as possible in the dark, as the secondary antibody is fluorescent.

9. After incubation, wash the cells twice.
10. Transfer the cells to flow cytometry tubes, by resuspending the cells 200ul staining buffer and moving them to the flow cytometry tubes on by one
11. Centrifuge the tubes for 5 minutes, at 300g, RT, and discard the supernatant afterwards
12. Resuspend the pellet in 100 ul dPBS and measure on the cytoflex
13. Analyze data in FlowJo

Maxwell RNA isolation

This is a simplified version of the official Maxwell RNA isolation protocol from the kit.
https://www.npchem.co.th/attachments/view/?attach_id=293376

Prepare before starting:
HB solution: Add 20 ul 1-Thioglycerol per 1 ml of Homogenization Solution.

Harvest the samples:
1. Wash the cells once with PBS and discard the PBS
2. Add 200 ul pre-chilled HB to each well, homogenize them with the pipet
3. Place the samples in RNase free 1.5 ml tubes on ice.

Prepare Maxwell for isolation:
1. Place the cartridge (RNA LEV Simple) in the black holder
2. Strip off the covers
3. Place plungers in position 8
4. Add 5 ul DNase (stored at -20) to position 4 (yellow solution), and the solution will turn green
5. Place 0.5 ml tubes (from the kit!) in the FRONT row (firmly press tubes)
6. Add 50 ul RNase free water in the 0.5 ml tubes (Check if there are NO air on the bottom of the tubes)

.
Lyse the samples:
1. Add per sample 200 ul lysis buffer and vortex immediately for 15 seconds.
2. Pipet the sample straight in its position in the RNA cartridge.

Start Isolation:
1. Turn on the Maxwell click RUN
2. Choose program 1 RNA Simply RNA
3. Choose Run (green button)
4. Open the door
5. Place the cartridge in position
6. Start

RNA quantification
1. Take tubes out of cartridge when program is finished
2. Gently mix tubes by tapping on the bottom and short spin on centrifuge
3. Pipet 2x 2ul nuclease free water on the biotek take 3 and do quality control
4. Now pipet your rna samples onto the take 3 and run to get RNA concentration (ng/ul). Pipet from the top of the sample!
5. Use this data to calculate the ul (volume) needed to have 1ug RNA. (1000 divided to the ng/ul number).

Protocol RNA -> cDNA conversion

Materials

- Small PCR tubes with attached lids (strip tubes)
- 1.5 ml tube for nuclease-free water
- 1.5 ml tube for RT (reverse transcription) mix
- Box containing RT reagents (from freezer)
- RNA isolates (stored -80)

Important Notes

- Always wear gloves, including when handling RNA isolates from the freezer.
- Work RNase-free and keep reagents on ice unless otherwise stated.

Procedure

1. Thaw RNA samples from the −80 °C freezer on ice.
   Thaw RT reagents as follows:
   - Thaw buffer and random hexamers at room temperature
   - That the rest on ice
2. Ensure all reagents are completely thawed before use.
3. Gently mix RNA samples (tap the tube with a finger) and briefly spin down to collect contents at the bottom.
4. Label the strip tubes according to the sample names.
5. Pipette the required volume (see results RNA isolation) of RNA from the top layer of each RNA sample into the corresponding labeled strip tube.
6. Add the specified volume (see results RNA isolation) of nuclease-free water to each RNA tube and seal with the strip cap.
7. Briefly spin down the RNA + water mix.
8. Visually check that all tubes contain approximately equal volumes.
9. Prepare the RT master mix:
   - Vortex all reagents except enzymes briefly before adding them to the RT mix tube.
   - Gently mix the complete RT mix.
10. Add 10 µl of RT mix to each RNA + water tube.
11. Briefly spin down the tubes again (ensure the centrifuge is balanced).
12. Place the sample strip into the thermocycler.
    Select:
    - Home → cDNA → Protocol
    - Confirm volume: 20 µl
    - Confirm cycling conditions:
      - 10 min at 20 °C
      - 30 min at 42 °C
      - 10 min at 20 °C
      - 5 min at 99 °C
      - 5 min at 20 °C
13. After the run, briefly spin down the tubes and store cDNA at −20 °C.

RT mix:

	1 sample	1 (inc standard curve)	18 (inc standard curve)
RT buffer	2ul	4ul	72ul
dNTP mix (10mM)	0.1ul	0.2ul	3.6ul
Rnasin	0.25ul	0.5ul	9ul
Rev transcriptase	0.5ul	1ul	18ul
Random hexamers	0.5ul	1ul	18ul
RNA	0.5ug	1ug	18ug
H20	1.65ul	3.3ul	59.4ul

qPCR Protocol

Note: This protocol is based on 8 samples (run in triplicate) and a standard curve with 8 dilution points, using a cDNA mix with a total volume of 20 µL.

Materials:

- One PCR strip for the standard curve
- One PCR strip for the samples
- 1.5 mL tube for Taq master mix
- 1.5 mL tube for primer mix

Procedure:

1. Thaw the cDNA, forward primer, reverse primer, and SYBR Green master mix (on ice).
2. Label a new PCR strip for the standard curve (STD4 to STD0.125).
   Label a second PCR strip for the samples, including negative control (NC) and positive control (PC).
   Label tubes for the Taq master mix and the primer mix.
3. Mix the cDNA strip, and briefly spin down.
4. **Dilute cDNA samples**: Transfer 10 µL of each cDNA sample to the labeled sample strip (including NC and PC), and add 120 µL of RNase-free water.
5. **Pool remaining cDNA**: Combine the remaining volumes of all cDNA samples into a single tube labeled STD4.

6. **Prepare the standard curve as follows:**

Standard	**Volume used (µL)**	**RNAse-free water (µL)**
STD 4	80 µL pooled cDNA	120 µL
STD 2	80 µL of STD4	80 µL
STD 1	80 µL of STD2	80 µL
STD 0.5	80 µL of STD1	80 µL
STD 0.25	80 µL of STD0.5	80 µL

7. **Prepare primer mix (either for AP gene or housekeeping gene such as β-actin):**

- 20 µL forward primer (vortex before use)
- 20 µL reverse primer (vortex before use)
- 60 µL RNase-free water

8. **Prepare Taq master mix**: Vortex both SYBR Green and the prepared primer mix briefly before combining.
9. Briefly vortex and spin down all strips (samples, standard curve, and Taq master mix).
10. Pipette 2 µL of each standard (in triplicate) into the 384-well plate.
11. Pipette 2 µL of each diluted cDNA sample (in triplicate) into the 384-well plate.
12. For the **negative control (NC)**, add 8 µL of Taq master mix and 2 µL of RNase-free water.
13. For the **positive control (PC)**, add 2 µL of cDNA known to be positive and 8 µL of Taq master mix.
14. Add 8 µL of Taq master mix to all wells (including standards, samples, NC, and PC).
15. Seal the plate with MicroAmp adhesive film, press down firmly, and centrifuge briefly at 1500 rpm (then stop immediately). Ensure all reagents are at the bottom of the wells.
16. Load the plate into the qPCR machine (ensure the correct orientation, with the camera symbol visible).

qPCR machine protocol:

Stage 1:	10 min 95℃
Stage 2:	15 sec 95℃ 30 sec 60℃ 40 cycli
Stage 3:	15 sec 95℃ 1 min 60℃ Gradient from 0.05/set to 95℃